HELIOTEK
A Division of TEXTRON Inc.
12500 GLADSTONE AVE., SYLMAR, CALIFORNIA 91342 · TWX 910-496-1488 · Area Code (213) 365-4611

Development of Lithium Diffused Radiation Resistant Solar Cells

FINAL REPORT PART I

By: P. Payne
L. Somberg

15 July 1970

JPL Contract No. JPL 952547

This work was performed for the Jet Propulsion Laboratory, California Institute of Technology, as sponsored by the National Aeronautics and Space Administration under Contract NAS7-100 .

Heliotek, Division of Textron Inc.
12500 Gladstone Avenue
Sylmar, California

This report contains information prepared by Heliotek, division of Textron Inc., under JPL subcontract. Its content is not necessarily endorsed by the Jet Propulsion Laboratory, California Institute of Technology, or the National Aeronautics and Space Administration.

SUMMARY

This report covers the first twelve months of progress on JPL Contract 952547 (June 17, 1969 - June 19, 1970).

TiAg, TiPdAg and Aℓ contact systems on P/N cells were evaluated for strength and humidity resistance. Contact strength tests were performed by soldering or ultrasonically welding tabs to the contacts and pulling at a 90° angle until failure. Both tab attaching methods were used to evaluate the TiAg and TiPdAg contacts. The soldered bonds withstood more than 500 grams pull (when the silicon did not fail) and the ultrasonically welded bonds withstood more than 150 grams pull. In both cases the pull strengths are comparable to those obtained with TiAg contacts on standard N/P cells, which also exhibit pull strength in excess of 500 grams for a soldered bond and 150 grams for an ultrasonically welded bond. Ultrasonic welding was used to attach 0.002" tabs to the Aℓ contacted cells and these bonds also withstood more than 150 grams pull, which as discussed in Section 2.2.1 is sufficient strength for reliable interconnection of cells.

Humidity testing of these three contact systems gave the following results: 1) TiAg front contacts peeled significantly (35% average) when tape tested after 100 hours of exposure to 95% relative humidity at 65° and peeled 100% after 200 hours exposure; 2) Aℓ contacts withstood 288 hours exposure before peeling occurred; then two out of ten cells exhibited peeling--30% of the bar on one cell and 80% of the bar on another cell; 3) one out of ten of the TiPdAg contacted lithium cells had approximately 20% of the bar peel after 288 hours.

BBr_3 was investigated as an alternative boron diffusion source, since the $BC\ell_3$ diffusion source presently used has two undesirable characteristics: 1) stresses are introduced into the silicon during the diffusion which would make it difficult to fabricate large area and thin lithium cells and 2) the etch reaction between the $BC\ell_3$ and silicon is a drawback in fabricating special cell types. The BBr_3 diffusion has been developed to the extent that high efficiency cells can be fabricated. To date, the I_{sc} (measured in AMO solar simulator) of BBr_3 diffused cells is typically 5 to 10% lower than the I_{sc} of $BC\ell_3$ diffused cells, which is typically 32 to 35 mA/cm^2; however, efficiencies greater than 11% have been obtained. The stresses have been eliminated and 0.006" thick 2 x 6 cm blanks have been diffused with no bowing.

Evaporation of lithium was investigated and a technique was developed to minimize post-evaporation oxidation. Lithium concentration profiles were similar to those obtained with the painted-on lithium mineral oil source. High efficiency lithium cells were obtained. Comparison of the cumulative frequency distributions for evaporated and painted lithium cells did show, however, that between 50 and 90% yield, the output fell off more rapidly for the cells with the evaporated source, such that at 90% yield the output of the evaporated lithium cells was 25.4 mW while the output of the painted cells was 26.4 mW.

Since regions of the cell with no lithium could affect post radiation output, an experiment was designed to evaluate the effect of varying the percentage of undiffused region. It was found that the undiffused regions did not affect the bulk resistivity or the lithium concentration profiles of the diffused regions. Also, no correlation could be drawn between lithium coverage and electrical output. These cells were delivered to JPL for radiation testing, which should indicate whether or not complete lithium coverage of the back cell surface is necessary for optimum cell recovery.

Eight hour lithium diffusions at 325°C were investigated. The crucible grown cells fabricated with these lithium diffusion parameters have shown some of the highest lithium cell efficiencies yet observed. The median output of one group of 60 cells was 30 mW (11% efficiency) with 10% of the cells having outputs ≥ 32 mW (11.8% efficiency) and 90% of the cells having outputs ≥ 27 mW (9.9% efficiency.

Seven lots (60 cells per lot) of lithium doped P/N solar cells have been fabricated and delivered to JPL for radiation testing and analyses by other laboratories. Statistical analysis of the cell outputs was performed for each lot of cells delivered. Significant improvements in cell efficiencies were made during the previous contract and particularly high efficiencies were obtained with crucible grown lithium cells.

During this contract further improvements have been made on crucible grown lithium cells by using an eight hour lithium diffusion at 325°C (Lot 3). The table below compares the maximum power cumulative frequency distributions at 10, 50 and 90% for Lot 10 on last year's contract and Lot 3 on the present contract. The values shown are for the same intensity at AM0 equivalent sunlight.

TABLE I

MAXIMUM POWER CUMULATIVE FREQUENCY DISTRIBUTIONS FOR CRUCIBLE GROWN LITHIUM CELLS.

Percentile	Lot 3	Lot 10
10%	32.0 mW	30.4 mW
50%	30.0 mW	28.3 mW
90%	27.0 mW	26.1 mW

The outputs shown for the Lot 3 cells correspond to efficiency range of 9.9% to 11.8% with a median efficiency of 11.0%. These same cells were irradiated and reported on by TRW, Inc. under JPL Contract 952554. They had efficiencies 11 to 20% greater than the output of 10 ohm cm N/P cells after being irradiated with 1 MeV electrons to an integrated flux of $3 \times 10^{15} e/cm^2$. The lithium cells had recovered outputs of 21.7 to 23.5 mW while the N/P cell output was 19.5 mW.

TABLE OF CONTENTS

Section	Description	Page
1.0	Introduction	1
2.0	Technical Discussion	2
2.1	Boron Diffusion Investigation	2
2.2	Contact Evaluation	15
2.3	Lithium Coverage	18
2.4	Lithium Evaporation	18
2.5	Eight Hour Lithium Diffusions	19
2.6	Room Temperature Storage of Lithium Cells	23
2.7	Cells Delivered to JPL	24
3.0	Conclusions	45
4.0	Recommendations	47

LIST OF FIGURES

Figure No.	Description	Page
1	Boron Diffusion System	3
2	I-V Characteristic of Diffusions Using BBr_3 in an Oxygen Ambient.	8
3	I-V Characteristic Curves of 1 ohm cm P/N Cell Diffused with BBr_3 Source	12
4	I-V Characteristic Curve of a Lithium Cell Fabricated with a BBr_3 Diffusion	14
5	Effect of Humidity on Aluminum Contacted P/N Cells	17
6	Maximum Power Distributions of Lithium Cells	20
7	Concentration Profiles for Eight-Hour Lithium Diffusions at 325°C	22
8	Short Circuit Current Distribution of Lithium Cells Fabricated for the Second Lot	25
9	Maximum Power Distribution of Lithium Cells Fabricated for the Second Lot	26
10	Short Circuit Current Distribution of Lithium Cell Fabricated for the Fifth Lot	28
11	Maximum Power Distribution of Lithium Cell Fabricated for the Fifth Lot	29
12	Short Circuit Current Distribution of Lithium Cells Fabricated for the Sixth Lot	30
13	Maximum Power Distribution of Lithium Cells Fabricated for the Sixth Lot	31
14	Short Circuit Current Distribution of Lithium Cells Fabricated for the Seventh Lot	33
15	Maximum Power Distribution of Lithium Cells Fabricated for the Seventh Lot	34
16	Short Circuit Current Distribution of Lithium Cells Fabricated for the First Lot	35
17	Maximum Power Distribution of Lithium Cells Fabricated for the First Lot	36
18	Short Circuit Current Distribution of Lithium Cells Fabricated for the Third Lot	37
19	Maximum Power Distribution of Lithium Cells Fabricated for the Third Lot	38
20	Comparison of Float Zone and Crucible Grown Lithium Cells Diffused Eight Hours at 325°C	40
21	20 ohm cm Crucible Grown Lithium Cell Before and After Irradiation	42
22	20 ohm cm Crucible Grown Lithium Cell Before and After Irradiation	43
23	Lithium Cells Versus 10 ohm cm N/P Cell	44

1.0 INTRODUCTION

The goal of this contract was to investigate the effect of various process parameters on lithium doped solar cell performance. This program was a continuation of work done on JPL contract 952247, and it was organized into three areas of study. The three basic areas included P-N diffusion studies, lithium diffusion studies, and contact studies.

The purpose of the P-N diffusion studies was to develop a boron diffusion which: 1) did not etch silicon, 2) would yield higher efficiency lithium cells due to reduced stresses and 3) could be used for larger area and thinner cells (also due to reduced stresses).

The lithium diffusion studies were directed toward improving cell efficiency and obtaining maximum radiation damage recovery. Radiation studies conducted under JPL contract by other laboratories had shown in one limited experiment that long lithium diffusions done around 325°C resulted in higher efficiency and more radiation resistant lithium cells. These diffusion parameters as well as the process techniques of complete lithium coverage of the back cell surface and lithium evaporations were used in fabricating the cells that showed unusually good radiation recovery, so these same parameters were further investigated in this program in order to determine whether these results could be reproduced.

The contact studies included evaluation of the Ti-Ag contacts presently used as well as investigation of other contact metals such as Pd and Al.

In addition to the experimental studies, lithium doped solar cells were fabricated and sent to JPL for radiation testing and analysis by various radiation laboratories.

2.0 TECHNICAL DISCUSSION

2.1 BORON DIFFUSION INVESTIGATION

Boron trichloride (BCl_3) is the dopant source typically used for standard boron diffusions at Heliotek. High output cells are obtained with this process; however, certain characteristics of this diffusion are undesirable. The stresses introduced into the silicon with this diffusion are not usually a problem with the small 1 x 2 cm blanks, but as the cell size is increased or the cell thickness decreased the stresses result in a larger percentage of bowed cells.

In addition, silicon is etched during this diffusion. This is a drawback in fabricating special cell types such as the cell with a stable N^+ region at the junction. The purpose of the N^+ region is to maintain the majority carrier concentration and, consequently, good junction characteristics as the lithium is depleted by reaction with radiation defect sites. The N^+ region is obtained with a phosphorous diffusion and then the cell is processed according to standard lithium cell fabrication techniques. Use of BCl_3 as the boron diffusion source, with its variable etch rate, has made it impossible to fabricate this special cell with a controlled width on the phosphorous region. The variable etch rate and introduction of stresses were the primary reasons for investigating other sources.

Previous work has included investigation of B_2H_6, BN and Borofilm, but they were not included in present contract work.

BBr_3 has been successfully used by other semiconductor laboratories and it was the source which was investigated during this contract period. A schematic of the diffusion system is illustrated in Figure 1. This diffusion is usually performed in an oxidizing atmosphere with the O_2 reacting with the BBr_3 to produce B_2O_3,

$$4BBr_3 + 3O_2 \longrightarrow 2B_2O_3 + 6Br_2 \qquad \text{Eq. 1}$$

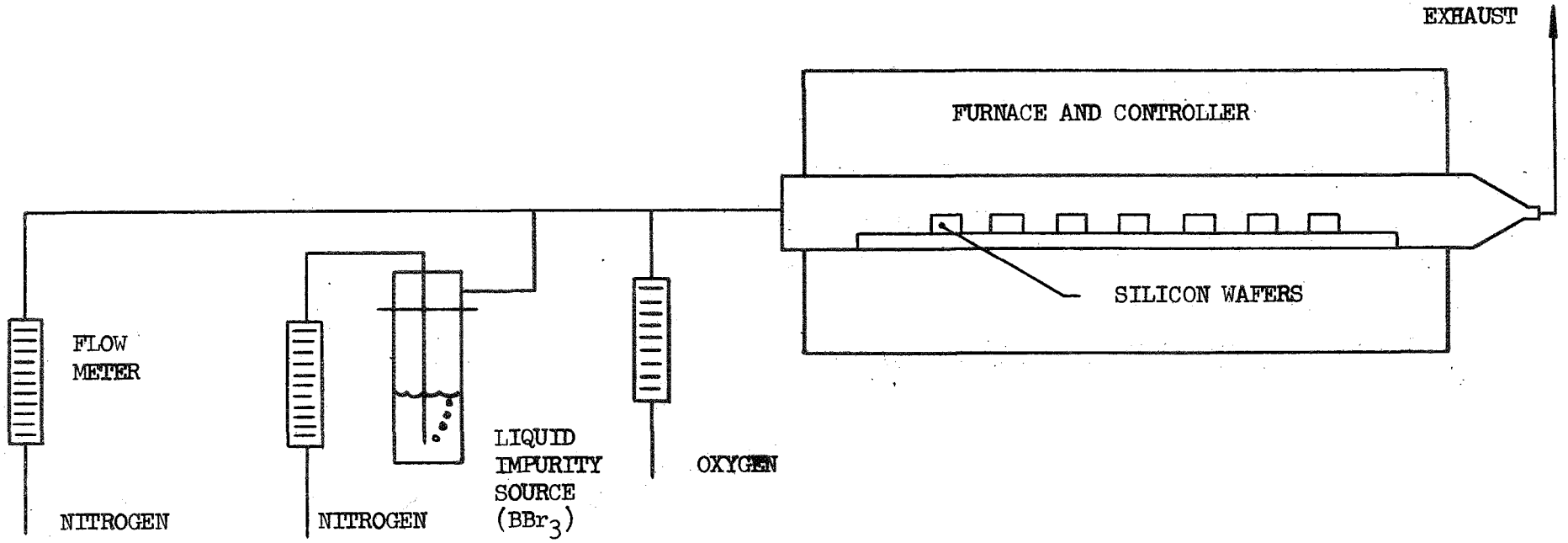

DIFFUSION SYSTEM USING A LIQUID IMPURITY SOURCE

Figure 1

which deposits on the slices as a glass layer. The O_2 also reacts with the silicon to form its oxide,

$$Si + O_2 \rightleftharpoons SiO_2 \qquad \text{Eq. 2}$$

The B_2O_3 reacts with silicon to form elemental boron,

$$3Si + 2B_2O_3 \rightleftharpoons 3SiO_2 + 4B \qquad \text{Eq. 3}$$

which diffused into the lattice to form the P-N junction. For each of the above reactions the equilibrium constant (K) and Gibb's free energy were calculated at the temperature at which the diffusion is performed ($1328^{\circ}K$) to note which reactions occur and if they proceed to completion.

The standard free energy for a reaction from reactants to products at STP (standard temperature and pressure, $298^{\circ}K$ - 1 atm) can be found by the expression,

$$\Delta F^{\circ} = -RT\ln K \qquad \text{Eq. 4}$$

where

ΔF° = standard free energy change at STP
R = 1.987 cal/mole-$^{\circ}K$, ideal gas law constant
T = temperature ($^{\circ}K$)
K = equilibrium constant

Using the ΔF° values for each reaction, the equilibrium constants are calculated.

for Eq. 1: $\ln K_{298^{\circ}} = \dfrac{-(335.7\times10^{3}\ \text{cal/mole})}{-(1.987\ \text{cal/mole-}^{\circ}K)(198^{\circ}K)} = 505$

for Eq. 2: $\ln K_{298^{\circ}} = 325$

for Eq. 3: $\ln K_{298^{\circ}} = 27.7$

The expression providing the equilibrium constant as a function of temperature is given by the van't Hoff equation,

$$\frac{d\ln K}{dt} = \frac{\Delta H^\circ}{RT^2}$$

or by simple integration,

$$\ln K_T = \ln K_{298^\circ} + \frac{\Delta H^\circ}{R}\left(\frac{1}{298^\circ} - \frac{1}{T}\right) \qquad \text{Eq.5}$$

where T is the temperature of diffusion (1328°K) and ΔH° is the change in enthalpy for the reaction which must be determined at temperature T either by integration of the heat capacity (Cp) over the range 298° to 1328°K or from thermochemical tables(1).

The equilibrium constants were then determined for 1328°K. These in turn were substituted into the free energy reaction isotherm (eq. 4) and the free energy was calculated for this temperature. For all three reactions (eq. 1, 2 and 3) the values for ΔF at the temperature of diffusion satisfy the conditions for spontaneity (i.e., $\Delta F < 0$). The equilibrium constants obtained were comparable in magnitude to those at 298°K which indicates that the reactions proceed to completion at this high temperature.

Initial diffusions produced nonuniform glass layers as indicated by the interference pattern. Sheet resistance and hot point probe measurements indicated that the diffused layer was also nonuniform. The interference type glass layer as well as the nonuniform diffused layer indicated the existence of stratified laminar gas flow, and the following series of diffusions were performed to investigate this problem:

1) Diffusions were performed at three temperatures (900, 1055, 1125°C) to examine temperature effects on the laminar flow and glass pattern formation.

2) At each temperature, diffusion time, cell position, and gas flow, rates were varied to observe the effects of these parameters on cell performance.

(1) JANAF Interim Thermochemical Tables, Vol. 1,2,3, Dec. 1960, Thermal Laboratory, The Dow Chemical Co., Midland, Michigan.

2.1.1 Temperature Variation

In this experiment two groups of cells (10 cells/group) were diffused at each temperature mentioned above. One group was placed vertically and one horizontally in the diffusion boat. Identical diffusion times and gas flow rates were used in each case. It was determined by visual observation of interference layers that the glass layer on cells from diffusion at each temperature was nonuniform. The presence of this glass layer nonuniformity was independent of the horizontal or vertical positioning of the cells on the diffusion boat. However, the horizontal or vertical positioning of the cell did affect the pattern of nonuniformity in both the glass layer and the diffused region. The cells positioned vertically showed a high concentration P region at the top of the cell (as measured with a hot point probe which clearly shows differences in the impurity type, N or P, as well as gross differences in the impurity concentration) and an unconverted N region on the lower half of the cell, with the highest concentration N region being the section of the cell which was in the diffusion boat slot during diffusion. The horizontally positioned cells also had a nonuniform P layer with unconverted N regions; however the pattern was less definite. Variations in the sheet resistance of the P regions indicated that either the junction depth or concentration was also nonuniform. This experiment indicated that nonuniformity of the glass layer and diffused layer was independent of diffusion temperature.

2.1.2 Gas Flow Variations

When high nitrogen flow rates were used (1500 cm^3/minute) non-uniformity (as determined by visual observation of interference layers) in the glass layer was predominant. After glass removal an insoluble discoloration remained which could only be dissolved in an etchant that reacted with the silicon itself. When diffusions were made using nitrogen with no oxygen, an insoluble grey-black deposit resulted on the chemically-polished surface.

Using higher O_2 flow rates resulted in a uniform glass layer and its removal left no visible deposit. However, measurement with the hot point probe indicated that the diffusion was nonuniform--the N surface was not completely converted to a P region. By modifying the gas flow pattern the nonuniformity of the glass and diffused layers was reduced. The modification involved sealing the back end of the diffusion tube and having the gases enter and exhaust from the front end of the tube. This prevented the gases from streaming through the diffusion tube in stratified layers as was observed in the previous diffusion setup. With this modification, carrier and impurity gas flow rates were again varied. Once uniform glass and diffusion layers were obtained, the diffusion time was varied. The diffusion times producing the most desirable results with respect to high electrical characteristics or curve shape, were 10 and 85 minutes. Figure 2 shows the I-V curves measured in a tungsten light source (100 mW/cm^2) for cells diffused for these two time intervals. The cell diffused 10 minutes exhibited a soft knee characteristic but the values of the short circuit current and open circuit voltage were the highest achieved up to that time for any given diffusion. The 85-minute diffused cell had a curve factor which most closely approximated that obtained with a typical P/N junction using $BC\ell_3$ as the diffusion source. However, the short circuit current and open circuit voltage values were not optimum and repeat runs and slight process modifications with these particular diffusion parameters still did not result in high output P/N cells.

2.1.3 Diffusions without O_2

Some sets of parameters gave better results than others, but in the best cases the short circuit of cells diffused with BBr_3 in an oxidizing atmosphere were 10 to 20 mA lower than the short circuit currents of $BC\ell_3$ diffused cells. Consequently, BBr_3 was used without O_2 in a diffusion process similar to the $BC\ell_3$ to determine whether cells with comparable electrical characteristics (70 mA short circuit current, 600 mV open circuit, 30 - 33 mW maximum power) could be obtained.

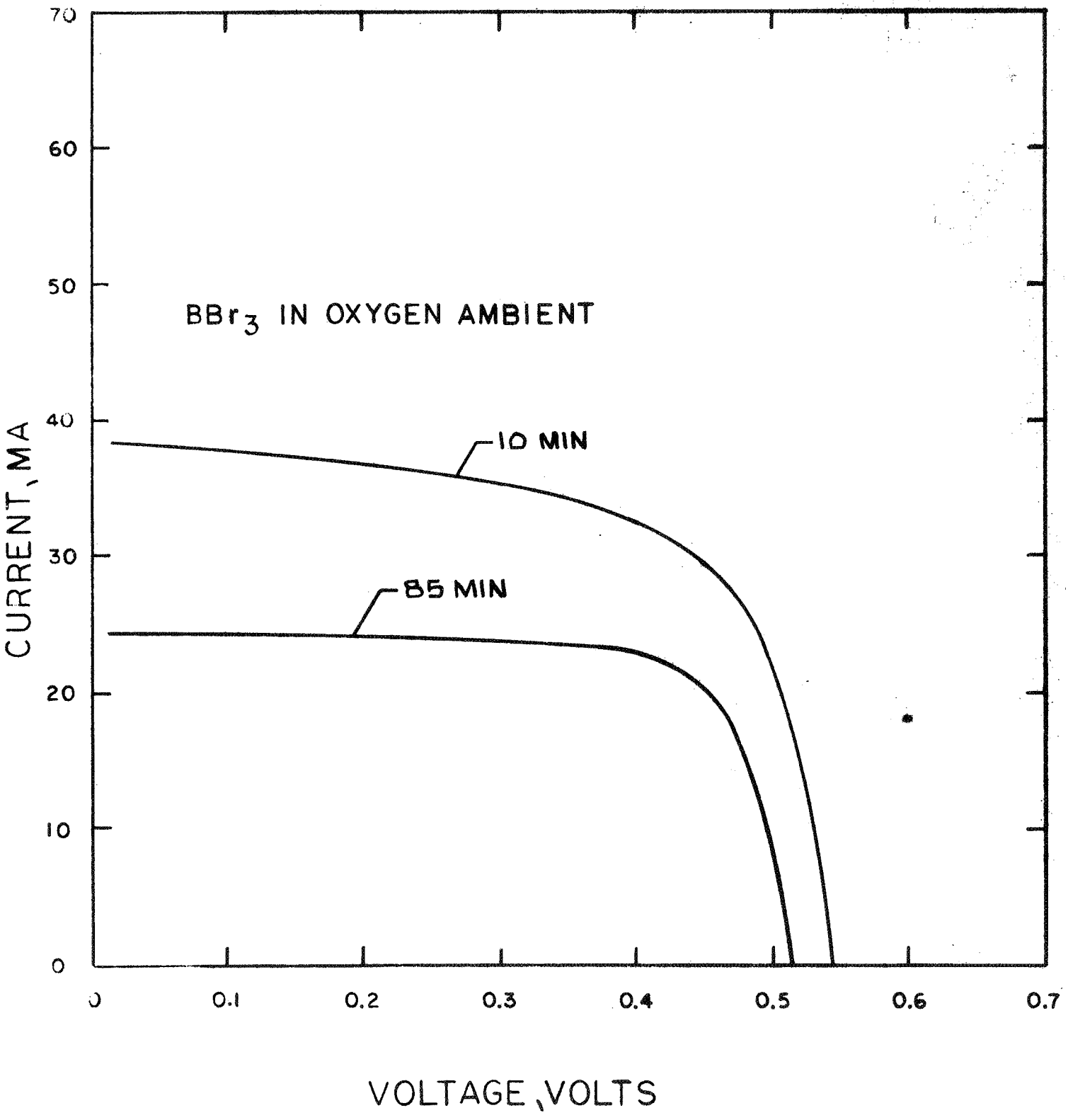

Figure 2. I-V Characteristic of Diffusions Using BBr_3 in an Oxygen Ambient. Measured at 25°C in a 100 mW/cm^2 tungsten light source.

In this process the BBr_3 vapor (rather than the boron oxide formed by the reaction of O_2 and BBr_3) becomes the local impurity and acts directly with the silicon cell blanks. Silicon is replaced in the reaction and a blank boron doped layer[2] is deposited on the cell surface according to the reaction,

$$4BBr_3 + 3\ Si \longrightarrow 3\ SiBr_4 + 4B \qquad \text{Eq. 6}$$

To determine if the reaction of equation 6 does indeed take place, calculations of the equilibrium constant (K) and Gibb's free energy (ΔF) were made, using equations 4 and 5.

For the reaction of equation 6,

$$\ln K_{298^\circ} = \frac{\sum \Delta F^\circ(\text{Products}) - \sum \Delta F^\circ(\text{Reactants})}{-RT}$$

$$\ln K_{298^\circ} = \frac{(-185 \times 10^3 \text{ cal/mole})}{-1.987 \text{ cal/mole} - {}^\circ K)(298^\circ K)} = 312$$

Substituting the values for ΔH (JANAF Tables) into equation 5, the equilibrium constant is obtained at $1328^\circ K$.

$$\ln K_{1328^\circ} = 312 - \frac{29 \times 10^3 \text{ cal/mole}}{1.987 \text{ cal/mole} - {}^\circ K} \quad (2.6 \times 10^{-3}\ {}^\circ K^{-1})$$

$$\ln K_{1328^\circ} = 274 \text{ or } K = e^{274}$$

---

(2) Powell, C. F. Campbell, I. E., Gonser, B. W., "Vapor Plating," John Wiley & Sons, N. Y., 1955. p. 107

This value of K may now be substituted into equation 4 to solve for the free energy reaction isotherm at the temperature of interest.

$$\Delta F_{1328^\circ} = -RT\ln K_{1328^\circ} \begin{cases} \Delta F < 0 \text{ reaction spontaneous} \\ \Delta F > 0 \text{ reaction nonspontaneous} \end{cases}$$

$$\therefore \quad \Delta F_{1328^\circ} = (-1987 \text{ cal/mole} - {}^\circ\text{K})(1328^\circ\text{K})(274) = -723 \text{ Kcal/mole}$$

This calculated value for the free energy reaction isotherm does satisfy the condition for spontaneity at the temperature at which solar cell blanks are diffused. Similarly it can be said that because of the very large value obtained for the equilibrium constant, the reaction proceeds to completion.

In addition to the reaction of equation 6, there is also the possible formation of silicon boride compounds of the form Si_xB_y (3). Due to the unavailability of the values of the chemical thermodynamic properties for these compounds, equilibrium constant and free energy calculations were not made. These boride compounds are suspected of being present in the typical black deposit found on the cell blanks surface, after diffusion, since this black layer reacts with hot HNO_3 and both SiB_3 and SiB_6 are black crystals which are soluble in HNO_3. The elementary boron which diffuses into the silicon crystal lattice to form the P-N junction probably originates from the reaction of equation 6 since the junction depth of about 3000-5000Å is considerably greater than the bond distances found in these boride compounds (something less than a few Angstroms).

---

(3) Powell, C.F. Campbell, I.E., Gonser, B.W., "Vapor Plating," Chp. 5 John Wiley & Sons, N.Y., 1955.

The resulting short circuit current for 1x2 cm cells measured in a 100 mW/cm^2 tungsten light source ranged from 55 to 60 milliamps. This was comparable to cells diffused with $BC\ell_3$. In addition, it was discovered that though BBr_3 etched the cell surface and a heavy boron layer formed, the problem of bowed cells due to stressed silicon was less severe with the BBr_3. Large area (2x2 cm and 2x6 cm) cell blanks were diffused and then placed on an optical flat to measure the gap created by a bowed slice. There was no measurable gap even in the case of the 2x6 cm blanks. When the 2x6 cm blank thickness was reduced to 0.006", there was still no measurable gap.

Figure 3 shows the I-V curves measured in both tungsten and solar simulator light sources for a 1 ohm cm crucible grown cell diffused with a BBr_3 source without O_2 gas. The cell characteristic curve indicated that a good P/N junction was formed. The short circuit current, open circuit voltage, and maximum power measured at 25°C in a 100 mW/cm^2 tungsten light source were as good as the characteristics of a $BC\ell_3$ diffused cell. The AMO output, however, was low due to low short circuit. The ratio of the short circuit currents, simulator to tungsten, was 1.10 or approximately 7% lower than a typical value of 1.18. This low ratio could have been due to a deeper junction in the BBr_3 diffused cells or an improper match of the antireflection coating to the AMO solar simulator spectrum. Since the diffusion time and temperature for the BBr_3 and $BC\ell_3$ diffusions were similar, as were the measured sheet resistances, it did not seem likely that a deeper junction existed in the cells diffused with BBr_3. However, the surface layer of the BBr_3 diffused cells was uneven in color, such that uneven antireflection coatings were also obtained; therefore it seemed probable that an improper match of the antireflection coating on parts of the cell surfaces to the AMO solar spectrum was the cause for the low simulator short circuit current. Even with the low short circuit current, the cell shown in Figure 3 had an AMO efficiency of greater than 11%.

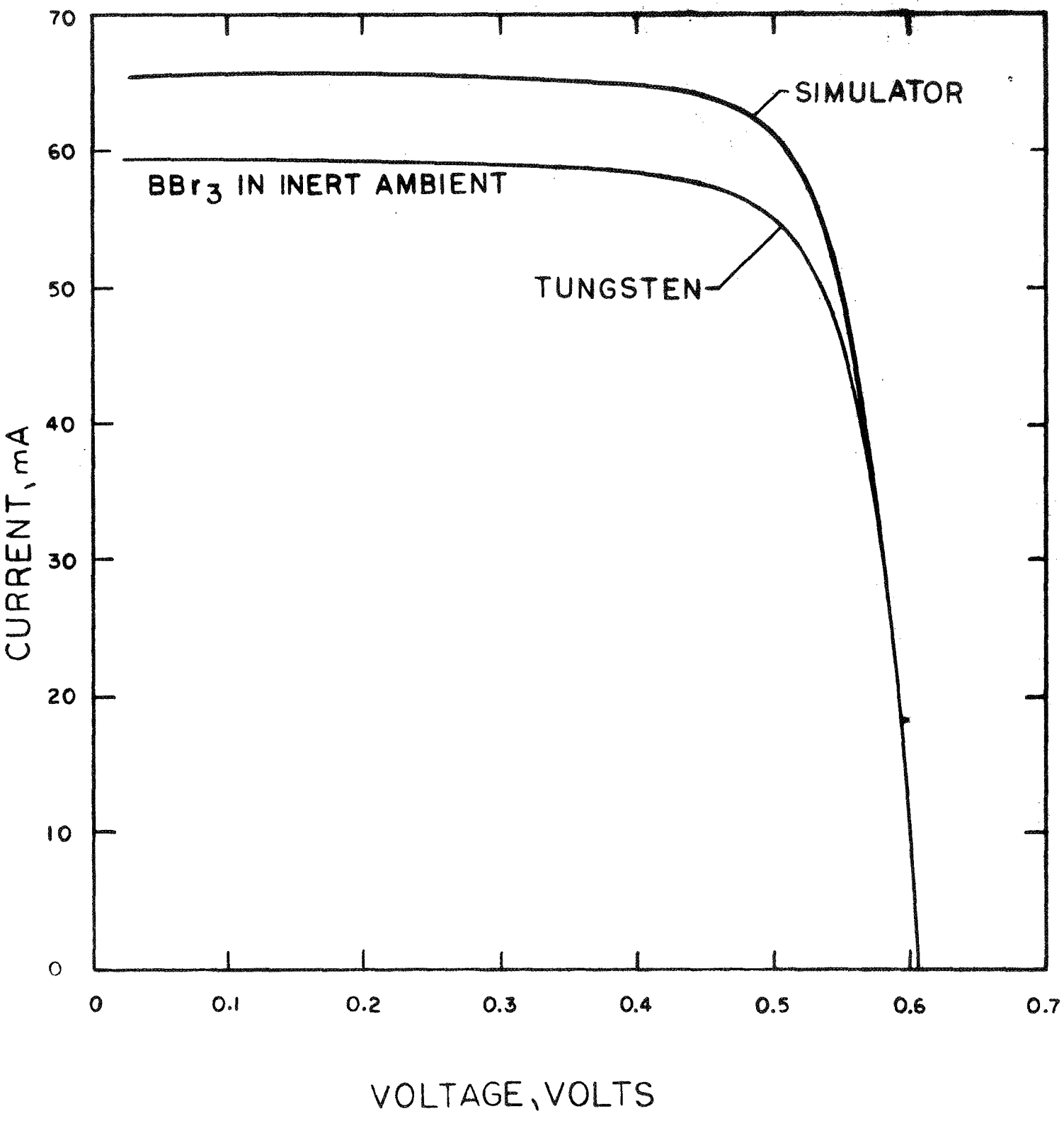

Figure 3. I-V Characteristic curves of 1 ohm cm P/N cell diffused with BBr_3 source.

The 20 ohm cm crucible grown 2x2 cm and 2x6 cm cells also showed good tungsten output but low simulator output. The AMO short circuit current for a 1x2 cm cell equivalent was approximately 6 mA low--64 mA instead of the 70 mA normally obtained with $BC\ell_3$ diffused cells.

In addition to standard P/N cells, lithium doped P/N cells (2x2 and 2.[illegible] cm in size) have been fabricated using the BBr_3 diffusion. The short circuit current for a 2x2 cm cell ranged from 123 to 129 mA. The curve factors for a number of these cells was low due to series resistance greater than 1 ohm; however, one of the better cells had a power output of 58 mW, which is equivalent to an efficiency of 10.9% (see Figure 4).

Since etching of silicon occurs in the BBr_3 diffusion without O_2, this diffusion is not suitable to use in fabricating special cell types which require a nonetching boron diffusion source. However, it does eliminate the problem of stresses encountered with the $BC\ell_3$ diffusion of large area and thin cells.

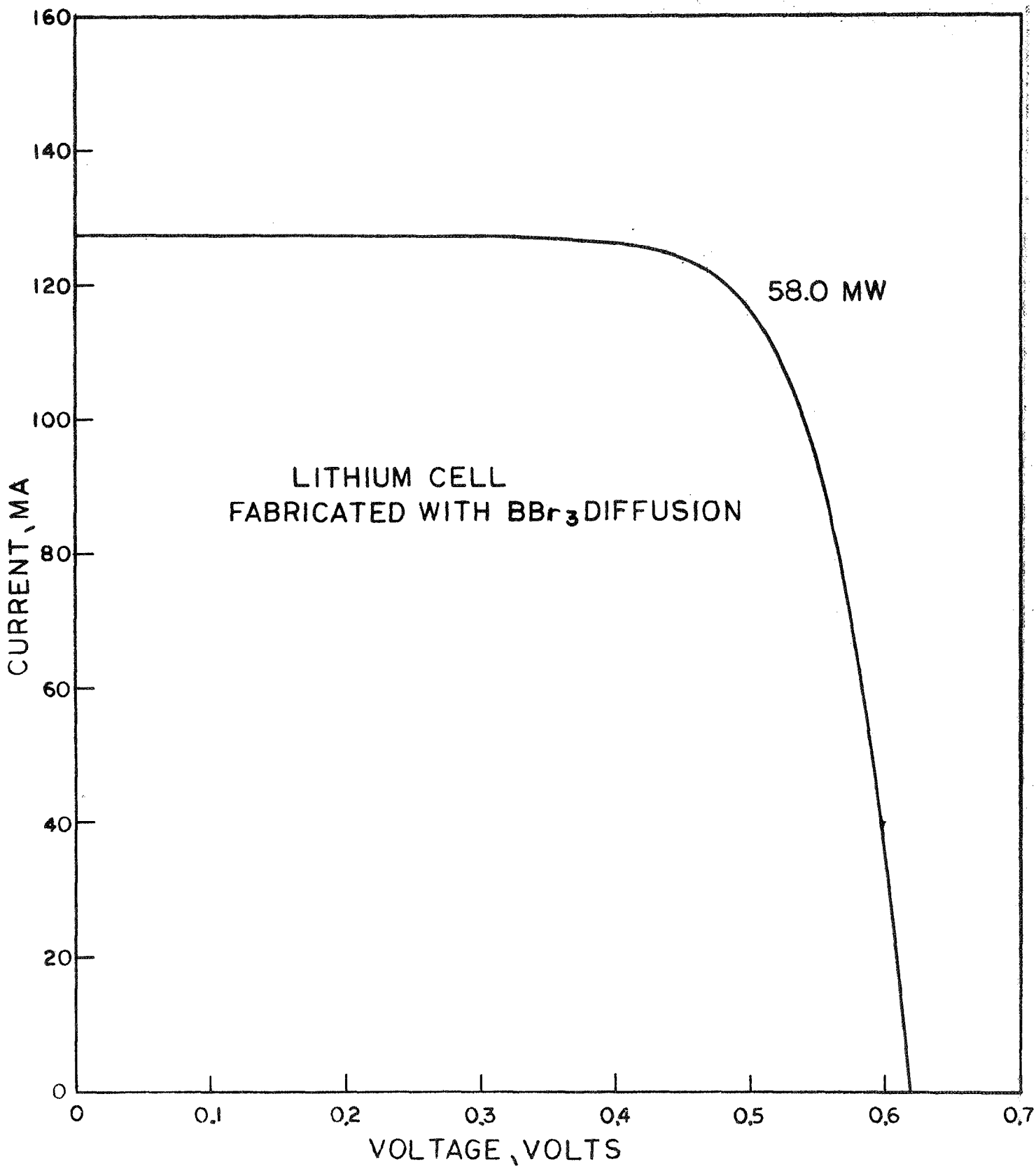

Figure 4. I-V Characteristic Curve of a Lithium Cell Fabricated with a BBr_3 Diffusion. 20 ohm cm crucible grown cell lithium diffused 90 minutes and redistributed 120 minutes at 425°C; measured in solar simulator at 140 mW/cm^2.

2.2 CONTACT EVALUATION

Humidity and peel tests were performed to evaluate the TiAg contacts presently used on lithium cells. TiPdAg and Aℓ contact systems on lithium cells were also included in this contact evaluation.

2.2.1 Peel Test

Peel tests (i.e. wired soldered or ultrasonically welded to the contact and pulled perpendicular to the cell surface until failure) were performed to determine the mechanical strength of the contact. In all cases where silicon fractures or divots did not occur, peel strengths in excess of 500 grams were obtained for TiAg and TiPdAg contacts.

The aluminum contact peel strength was tested by ultrasonically welding a 0.002" aluminum tab to the cell. The area of this bond was approximately one-eighth the area of a typical soldered bond and therefore peel strengths were lower. The peel strengths ranged from 180 to 270 grams. These peel strengths were considered to be good for the following reasons:

1) Failure occurred when the tab material tore with the welded section remaining bonded to the contact.

2) Peel strengths of ultrasonic bonds to TiPdAg and TiAg contacted cells were also in the range of 180 to 270 grams. These same cells exhibited soldered bond peel strengths of more than 500 grams.

There was an unusually large percentage of soldered bond failures of less than 500 grams due to silicon fractures. For example, in the group of 15 cells with TiAg contacts, 81% of the failures were due to fractured silicon rather than failing contacts, and fractures of less than 500 grams accounted for 50% of the silicon fractures. It is unusual for conventional N/P cells to have silicon divots occur at these low values. These peel strength results gave further indication of the stresses present in P/N lithium cells. The stresses are presumed to be primarily due to the boron diffusion since the P/N cells with no lithium which were peel tested also had failures with silicon fractures at less than 500 grams.

2.2.2 Humidity Test

The humidity resistance of the various contact systems was also evaluated. TiAg, TiPdAg, and Aℓ contacted cells were subjected to 95% relative humidity at 65°C. A nondestructive tape peel test (using Scotch brand tape #810) was used to evaluate contact deterioration, so that the humidity test and electrical measurements could be continued as long as no blistering or peeling of the contact occurred. The TiAg contacts showed the least humidity resistance. After approximately 100 hours exposure an average of 35% of the front contacts peeled and some edge peeling occurred at the back contact. After 200 hours the front contacts on all cells peeled completely and an average of 15% of the back contact peeled. After 288 hours exposure, only one cell out of 10 with TiPdAg contacts showed any degradation; approximately 20% of the bar peeled. Two out of ten of the Aℓ contacted cells exhibited peeling after 288 hours: 30% of the bar on one cell and 80% of the bar on another cell. Though the TiPdAg and Aℓ contacts did degrade with humidity, their performance was superior to the TiAg contact.

The electrical measurements (performed in 100 mW/cm^2 tungsten light source) showed that the most significant loss factor for cells with TiAg contacts was at maximum power due to increased series resistance (as determined by measuring the change in the slope of the I-V curve at open circuit voltage). No electrical degradation of the TiAg contacted cells was measurable after 48 hours. However, the maximum power degradation after approximately 100 and 200 hours of humidity exposure was 4 and 5%, respectively.

The lithium cells with Aℓ contacts exhibited the following degradation after 244 hours: 0-3.3% for the current at 450 mV; 0-2.5% for the short circuit current; less than 1% for the open circuit voltage. After 288 hours, three out of nine of the Aℓ contacted lithium cells exhibited high series resistance as shown in Figure 5. The degradation of the lithium cells with TiPdAg contacts after 288 hours was approximately the same as the Aℓ contacted cells after 244 hours. TiPdAg contacted P/N cells without lithium generally showed less than 1% electrical degradation of I_{sc}, V_{oc}, P_{max} over the same period of humidity exposure. This seems to indicate that the lithium is moving around in the bulk of the cell or is reacting with the contact, either of which could change the output.

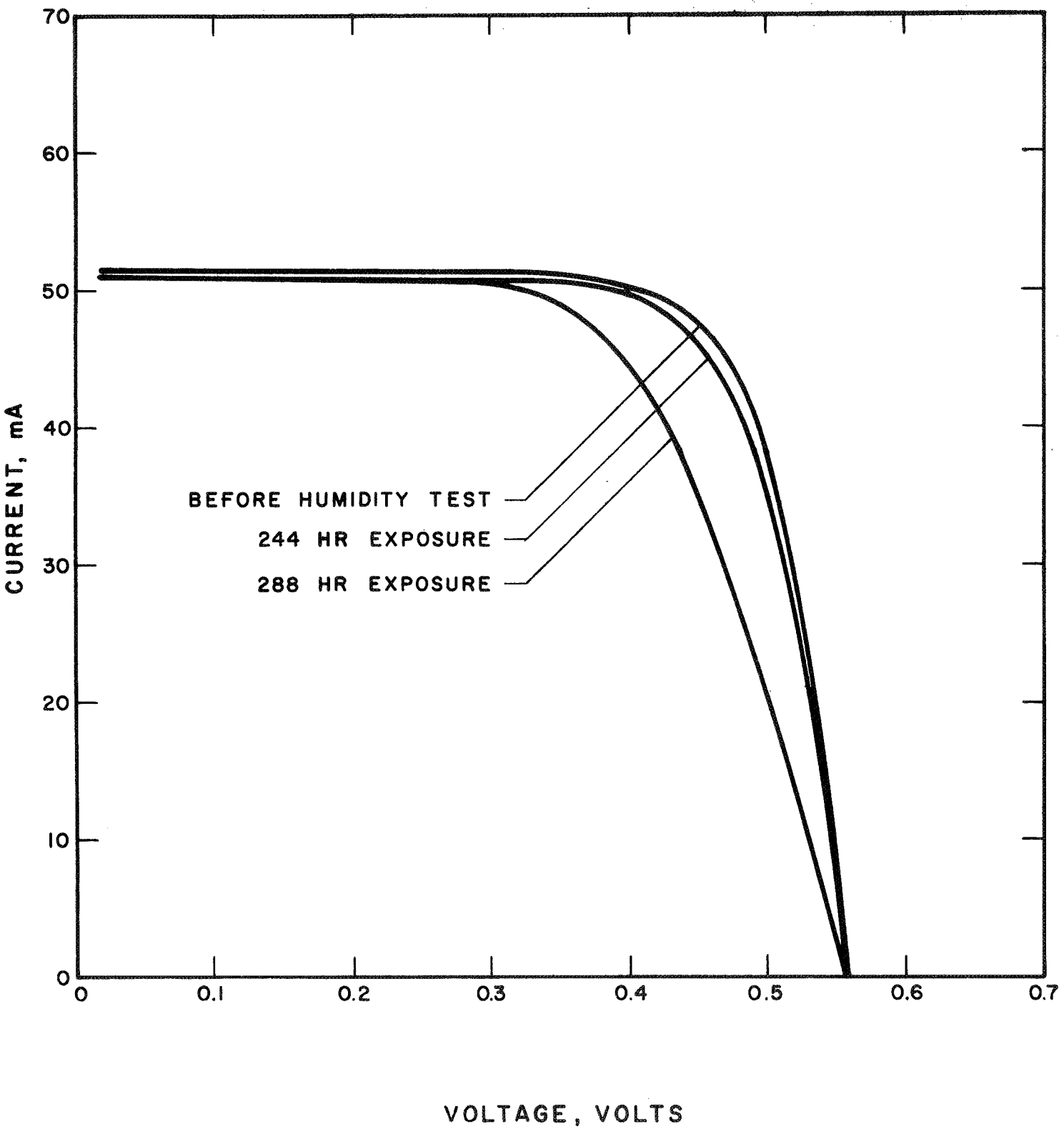

Fig. [illegible] Effect of Humidity on Aluminum Contacted P/N Cells. 95% Relative Humidity at 65°C; cell measured in 100 mW/cm² Tungsten Light source.

2.3 LITHIUM COVERAGE

It has been suggested that the percentage of the back surface which is covered with lithium should have an effect upon the radiation recovery characteristics of lithium cells. Cells fabricated by Heliotek have generally been painted with lithium so that the lithium source is always within 0.010 to 0.020 inches of the cell edge. This undiffused region around the perimeter of the cell, although small, could result in residual radiation damage. Lithium would not be present in this region to anneal damage sites and the junction edge effects might degrade the characteristic curve. An experiment was designed to evaluate the effect of varying the area of this region and the significance of this residual damage. Lithium was painted on three groups of cells (20 cells per group): the first group had 100% lithium coverage; the second, approximately 85%; and the third, approximately 50%.

Both boron diffused slices and undiffused silicon blanks were lithium diffused. The boron diffused slices were fabricated into cells to evaluate the electrical characteristics and the blanks were used for concentration profile analysis. The slice resistivity appeared to be independent of lithium coverage. Also, no clear correlation could be drawn between lithium coverage and cell output. The cells from this experiment were submitted to JPL for radiation testing. These radiation tests should indicate whether or not complete lithium coverage of the back cell surface is important in recovery of cells from radiation damage.

2.4 LITHIUM EVAPORATION

Evaporation of lithium as an alternative to painting on a lithium mineral oil suspension was investigated. Evaporation of lithium is desirable for several reasons: (1) it is less tedious and time consuming than the paint-on technique, (2) it is adaptable to a production line, and (3) there is no problem with the uniformity of the lithium layer on different parts of the same cell and from cell to cell.

Large diameter (0.125 inches) lithium wire was used as a source. This was handled far more easily than the lithium pellets which had previously been used in investigation of lithium evaporation. Oxidation of the lithium while opening the vacuum system was another problem area which had been encountered previously. This problem has been reduced by using helium, rather than air, to open the vacuum system after the lithium evaporation. The cells have been exposed to air during transfer from the vacuum system to the diffusion furnace but with apparently very little oxidation since cells have been obtained with the same sheet resistance and lithium concentration profile as cells with the painted-on lithium mineral oil source. Many of the cells with evaporated lithium had outputs as high as cells with the painted-on lithium. However, comparison of the cumulative frequency distributions for cells with painted-on versus evaporated lithium layers showed that there was more fall off in cell output and consequently a larger percentage of lower output cells with the evaporated lithium. Figure 6 shows the maximum power distribution as a function of lithium application for Lots 3 and 4. At a cumulative frequency of 90% there is a difference in output of about 1 mW for both lots.

2.5 EIGHT HOUR LITHIUM DIFFUSIONS

Eight-hour lithium diffusions at 325°C were investigated during this contract, since cells with this type of diffusion have been known to exhibit very high outputs. In the initial diffusions there were usually wide variations in electrical characteristics. The range in sheet resistance was much wider than that obtained with shorter diffusions at higher temperatures. It was also observed in these preliminary experiments that the sheet resistance was affected by the thickness of the lithium layer. This was unexpected since diffusion studies on a previous lithium cell contract had shown that decreasing the thickness of the lithium layer in order to reduce the pitting of the silicon in 90 minute diffusions at 425°C did not change the sheet resistance or the lithium concentration profile. In subsequent experiments with eight-hour

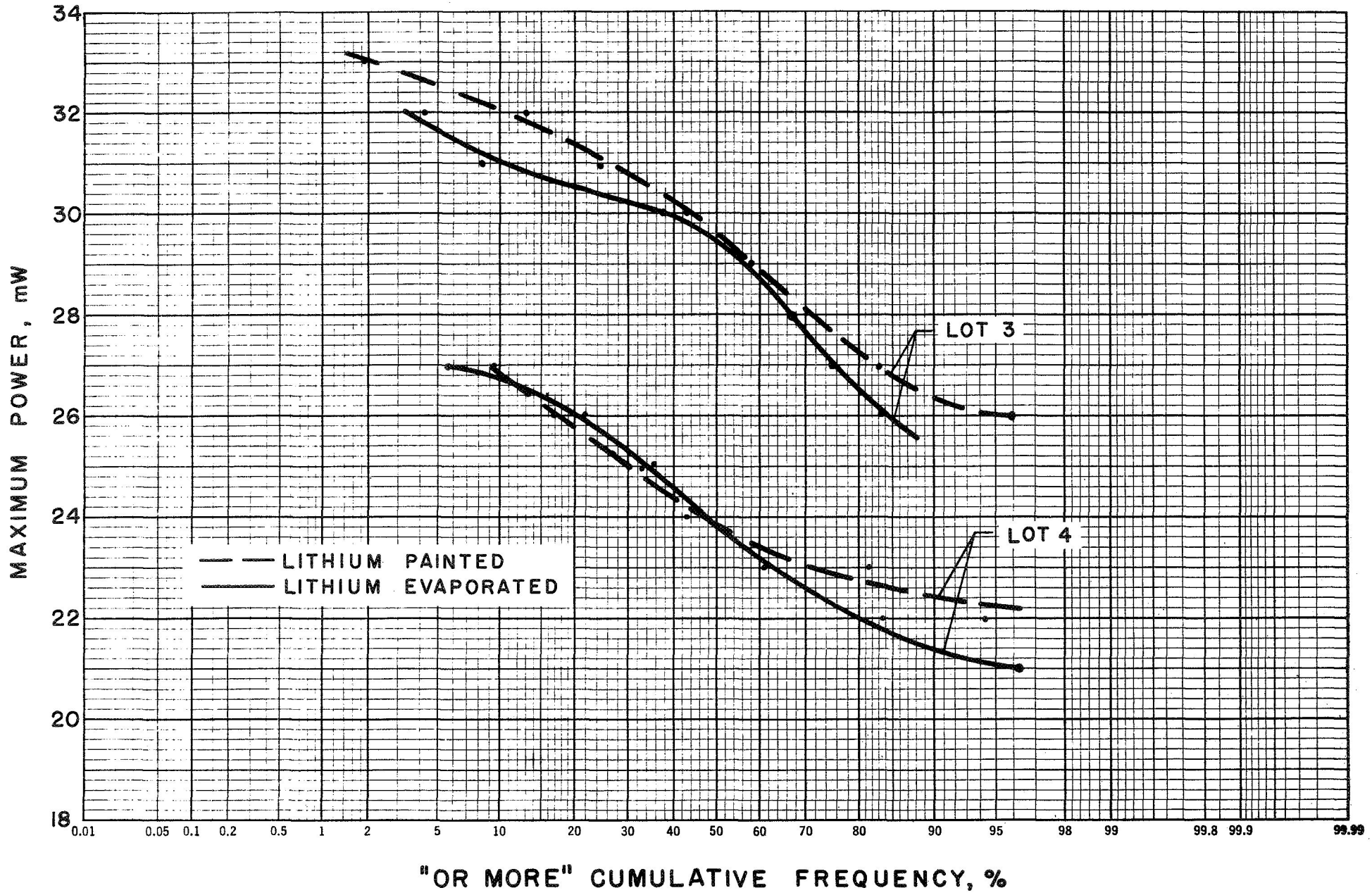

Figure 6. Maximum Power Distributions of Lithium Cells. Measured in solar simulator at 140 mW/cm^2.

lithium diffusions at 325°C, thicker lithium layers were investigated since silicon pitting during lithium diffusion is less severe as the diffusion temperature is decreased. The thicker lithium layers resulted in more uniform sheet resistances (still less uniform than sheet resistances of cells from conventional diffusions at 425°C) and did not cause severe pitting of the silicon.

Two lithium concentration profiles characteristic of the range of sheet resistance values typically obtained for an eight-hour diffusion at 325°C are shown in Figure 7 . The concentration profiles were determined by incremental lapping combined with sheet resistance measurements. Sheet resistance measurements were made using a four-point probe. It should be realized that the four-point probe measures the average resistance not the specific resistance of the surface region, so the calculations made reflect average concentrations throughout the cell. The steps in obtaining the concentration profile included:

1) Graphing I/V as a function of depth into the lithium diffused region and then calculating the Δ I/V for each 0.0005" increment

2) Calculating $\bar{N}\bar{\mu}$ as a function of depth into the lithium diffused region to the equation

$$\frac{d(I/V)}{dx} = Aq\bar{N}\bar{\mu} \qquad \text{Eq. 7}$$

where $d(I/V)dx$ = change in I/V over material x

A = conversion factor from Smits[4] for converting V/I readings to sheet resistance

q = electronic charge

$\bar{N}\bar{\mu}$ = average values of carrier concentration and mobility in the layer dx

3) Calculating $\bar{N}$ using average mobility ($\bar{\mu}$) values from Runyan[5].

---

4) Smits, F. M., "Bell Systems Technical Journal," 37, pp. 13-20, 1958.

5) Runyan, W. R., "Silicon Semiconductor Technology," McGraw-Hill 1965, p. 179.

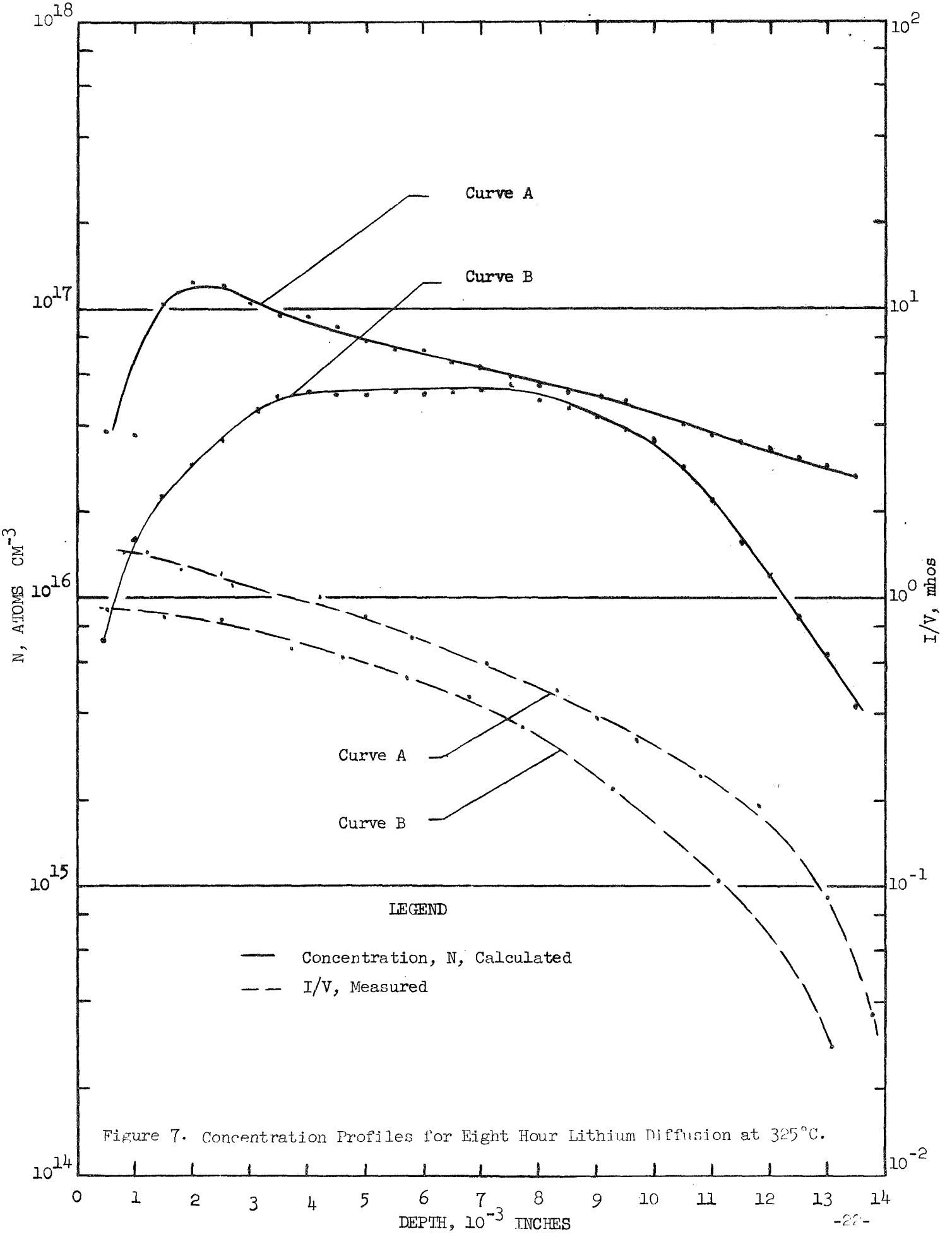

Figure 7. Concentration Profiles for Eight Hour Lithium Diffusion at 325°C.

Curve A represents cells with sheet resistances ranging from approximately 2.1 to 3.8 ohms/square and Curve B represents cells with sheet resistance from approximately 2.8 to 5.0 ohms/square. Comparison of this eight-hour diffusion to other lithium diffusions showed that the sheet resistances 2.1 to 3.8 ohms/square are in the same range as those from the 90 minute diffusion with 60 minutes redistribution at 425°C, and the sheet resistance from approximately 3.8 to 5.0 ohms/square are in the same range as those from a 90 minute diffusion with a 120 minutes redistribution at 425°C. The electrical output of some of these experimental cells diffused eight hours at 325°C was exceptionally good and is described in detail in Section 2.7.

2.6 ROOM TEMPERATURE STORAGE OF LITHIUM CELLS

The movement of lithium in the silicon lattice at room temperature could cause electrical instability in long-term storage. In order to evaluate this, seventeen cells fabricated in 1966 have been periodically measured. After $3\frac{1}{2}$ years storage at room temperature the following changes have occurred:

1) Six float zone cells (lithium diffused 90 minutes and redistributed 60 minutes at 425°C) were measured. Three of these cells which had exhibited approximately 10% power loss one year ago, have now degraded an additional 3%.

2) These three float zone cells had unusually large open circuit voltage decreases.

3) The other three float zone cells did not degrade in the same manner. Two of the cells showed 3 to 5% improvements in I_{sc} and P_{max} between October 1966 and March 1969; in the past year they have degraded 1 to 2% so they are still higher than they were initially. The third cell had the same output in 1969 as it did in 1966; in the past year it also degraded about 1% in the I_{sc} and P_{max}.

4) 100 ohm cm float zone cells lithium diffused 90 minutes and redistributed 60 minutes at 350°C, which one year ago showed a maximum of 1.84% I_{sc} degradation and 1.49% P_{max} degradation, now exhibit 2.0 to 3.7% total I_{sc} loss and 3.6 to 4.5% total P_{max} loss.

5) The crucible grown lithium cells (diffused 90 minutes and redistributed 60 minutes at 425°C) which showed 2 to 4% increase in output between October 1966 and March 1969 have shown degradation, but the outputs are still 1 to 2% higher than the initial outputs measured October 1966.

2.7 CELLS DELIVERED TO JPL

Seven lots of 60 lithium doped solar cells have been shipped to JPL for radiation tests in other laboratories. For each lot more than 60 cells were processed and tested so that a good selection for shipment could be made. Statistical analyses of the electrical output of each lot were performed.

Lot 2 consisted of 60 cells fabricated from 100 ohm cm Lopex silicon. They were lithium diffused 90 minutes and redistributed 120 minutes at 425°C. Figures 8 and 9 show the short circuit current and maximum power distribution for Lot 2 cells; 87 cells were included. Ten percent of the short circuit currents were ≥ 70 mA, 90% were ≥ 60.4 mA and the median was 64 mA. The median output was 25.4 mW; 10% of the cells had outputs ≥ 27.6 mW and 90% had outputs ≥ 23.4 mW. These cells showed the same variations in open circuit voltage previously observed with Lopex silicon. Some of the cells with high outputs had not only high short circuit currents, but also open circuit voltages of 570-580 mV. Some of the lower output cells had open circuit voltages as low as 540 mV. The cause is still uncertain. It could be dependent to some degree on oxygen concentration which some investigators have indicated varies considerably in Lopex silicon. At any rate, Lopex silicon seems to be the least predictable with respect to the output of lithium cells fabricated from it.

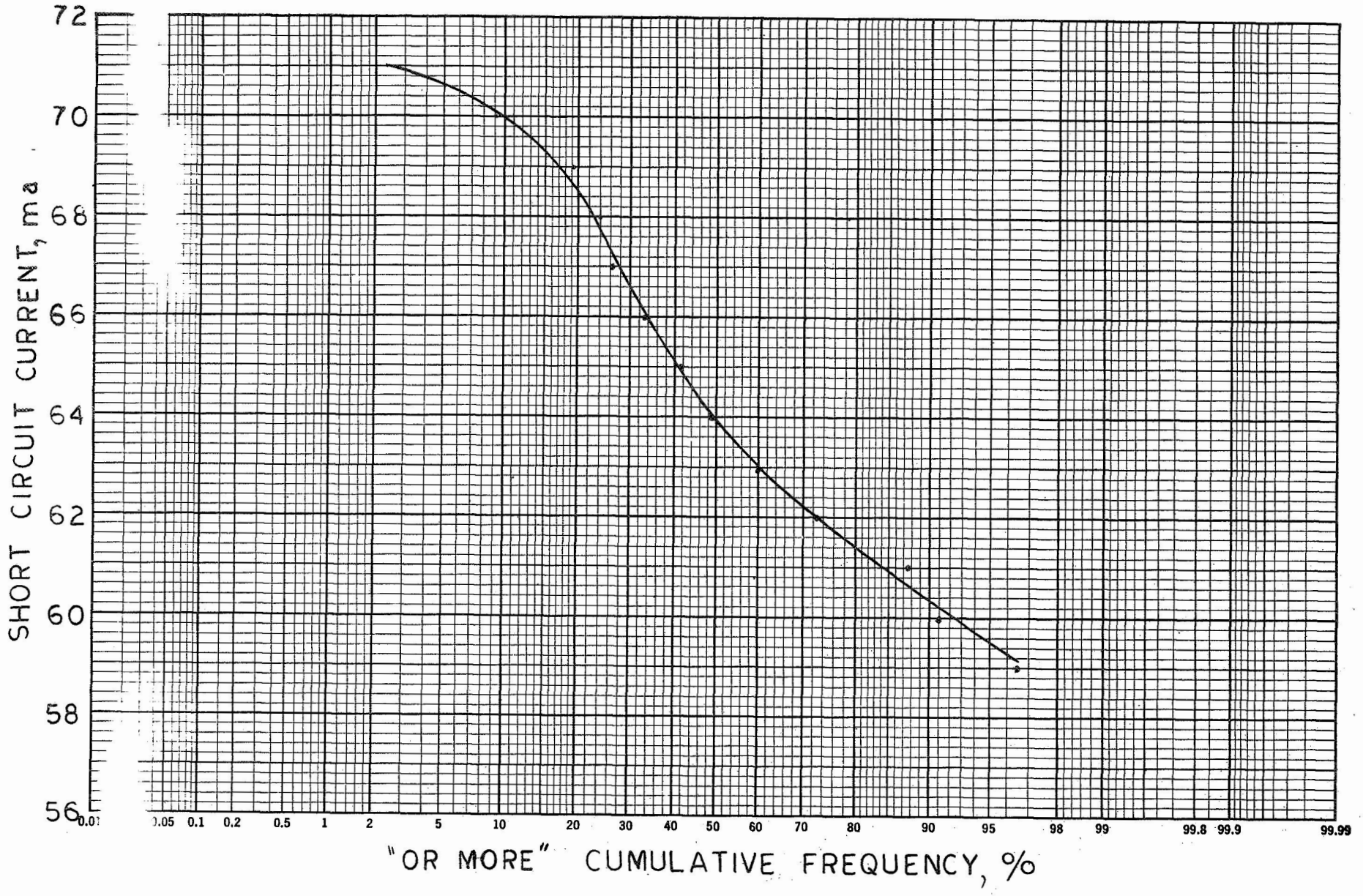

Figure 8. Short Circuit Current Distribution of Lithium Cells Fabricated for the Second Lot (87 cells). 100 ohm cm Lopex cells, lithium diffused 90 minutes and redistributed 120 minutes at 425°C; Measured at 25°C in solar simulator at 140 mW/cm^2.

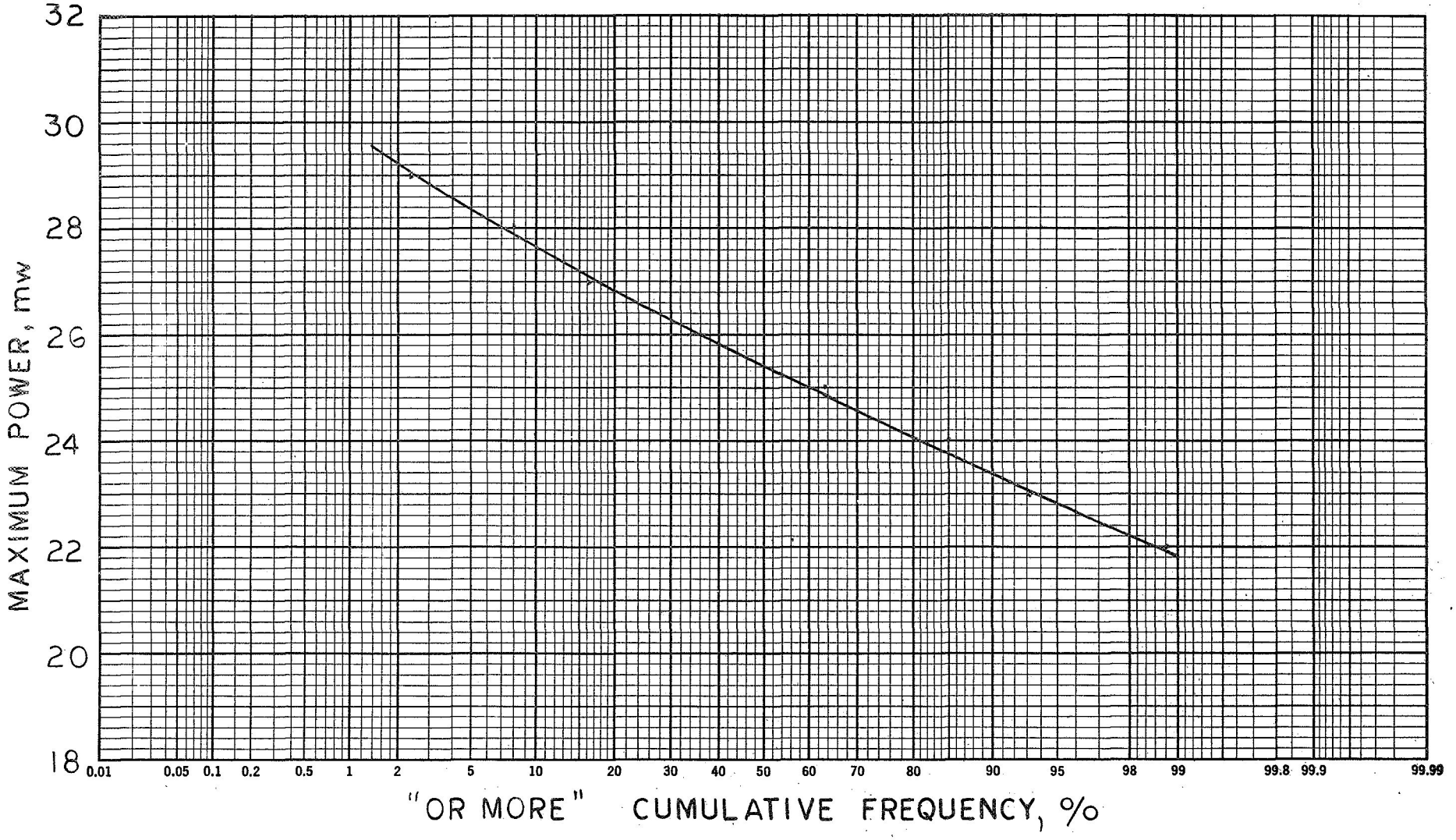

Figure 9. Maximum Power Distribution of Lithium Cells Fabricated for the Second Lot (87 cells). 100 ohm cm Lopex cells, lithium diffused 90 minutes and redistributed 120 minutes at 425°C; measured at 25°C in solar simulator at 140 mW/cm^2.

Lot 5 consisted of 30 float zone cells, lithium diffused 60 minutes and redistributed 120 minutes at 425°C, plus 30 experimental cells fabricated to determine the radiation recovery characteristics as a function of lithium coverage. Three variations in lithium coverage were used. For the first group the entire back surface was covered with lithium; the second group had approximately 85% of the surface covered with lithium, and the third group had only 50% of the surface covered with lithium. These cells, which were described earlier in the technical discussion, should provide information which indicates whether or not it is important to completely cover the back surface of the cell with lithium in order to obtain optimum recovery after radiation.

The maximum power and short circuit current distributions for the other 30 cells are shown in Figures 10 and 11. The 30 cells were selected from a group of 58 and all 58 were used for the distribution. The median short circuit current was 62.5 mA while 5% of the cells had short circuit currents ≥65.1 mA and 95% of the cells had short circuit currents ≥ 60 mA. The median output was 25.5 mW; 5% of the cells had outputs ≥ 27.0 mW and 95% had outputs ≥ 23.6 mW.

Lot 6 consisted of forty 20 ohm cm crucible grown cells, lithium diffused 90 minutes and redistributed 120 minutes at 425°C, as well as 20 experimental cells. The short circuit current and maximum power distributions for the crucible grown cells are shown in Figures 12 and 13. The spread in short circuit current is not too great, with only 10 mA change in the fifth to ninety-fifth percentile range. The median short circuit current was 65.7 mA, while 5% of the cells had short circuit currents ≥ 70.4 mA and 95% of the cells had short circuit currents ≥ 60.8 mA. With respect to maximum power 5% of the cells had outputs ≥ 30.2 mW while 95% of the cells had outputs ≥ 23.2 mW and the median output was 26.2 mW.

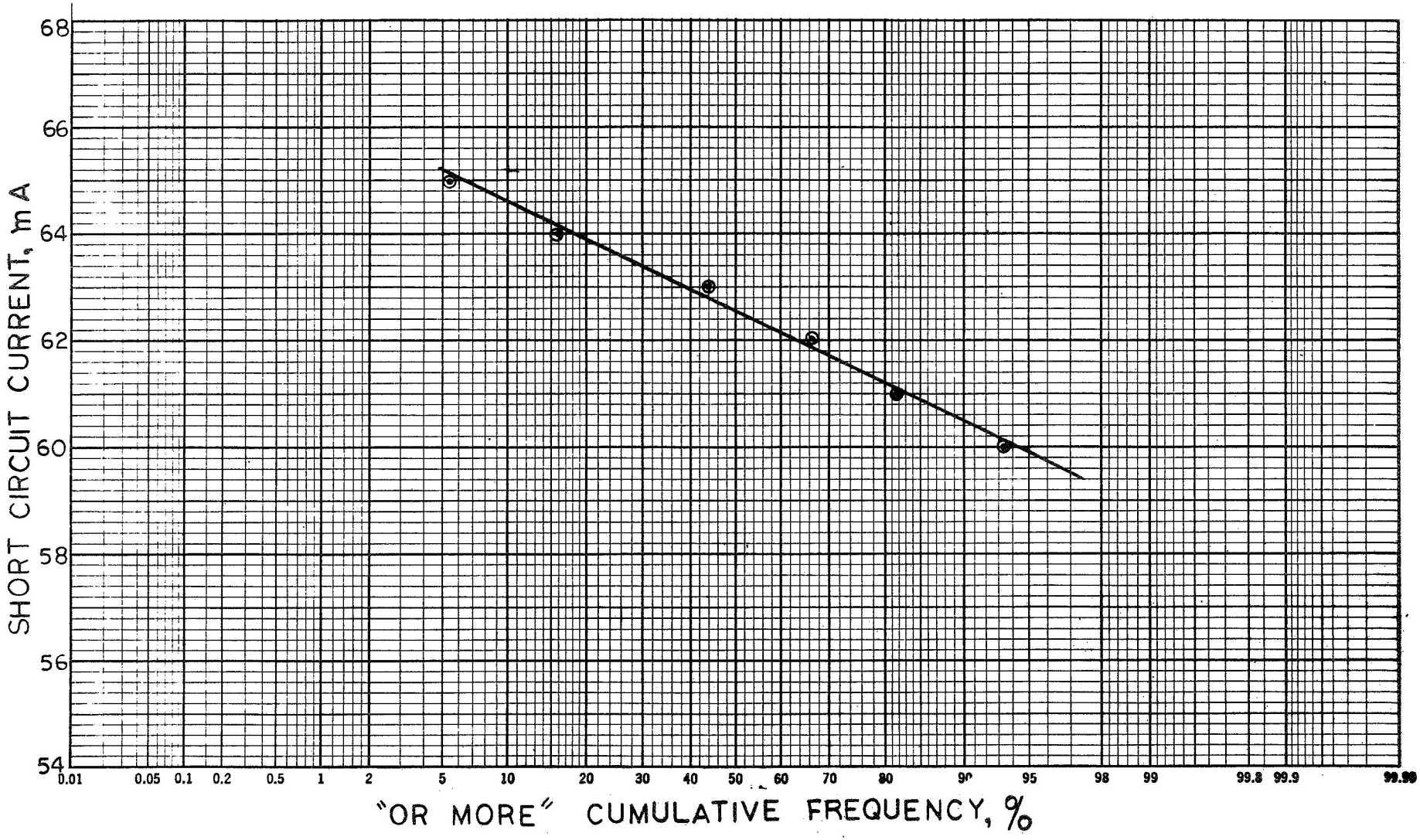

Figure 10. Short Circuit Current Distribution of Lithium Cells Fabricated for the Fifth Lot (58 Cells). 20 ohm cm float zone cells; lithium diffused 60 minutes and redistributed 120 minutes at 425°C; measured at 25°C in solar simulator at 140 mW/cm^2.

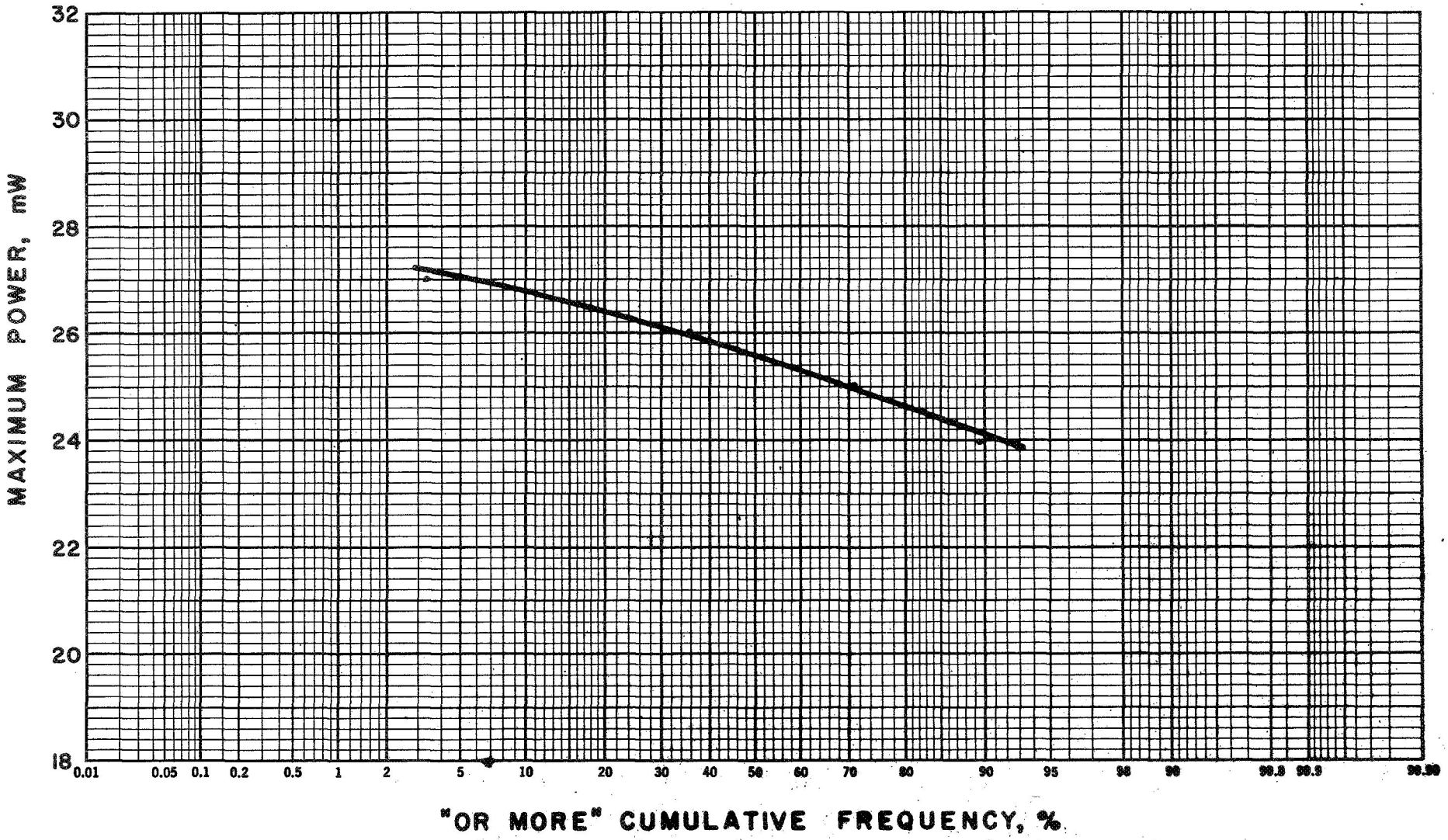

Figure 11. Maximum Power Distribution of Lithium Cells Fabricated for the Fifth Lot (58 Cells). 20 ohm cm float zone cells; lithium diffused 60 minutes and redistributed 120 minutes at 425°C; measured at 25°C in solar simulator at 140 mW/cm^2.

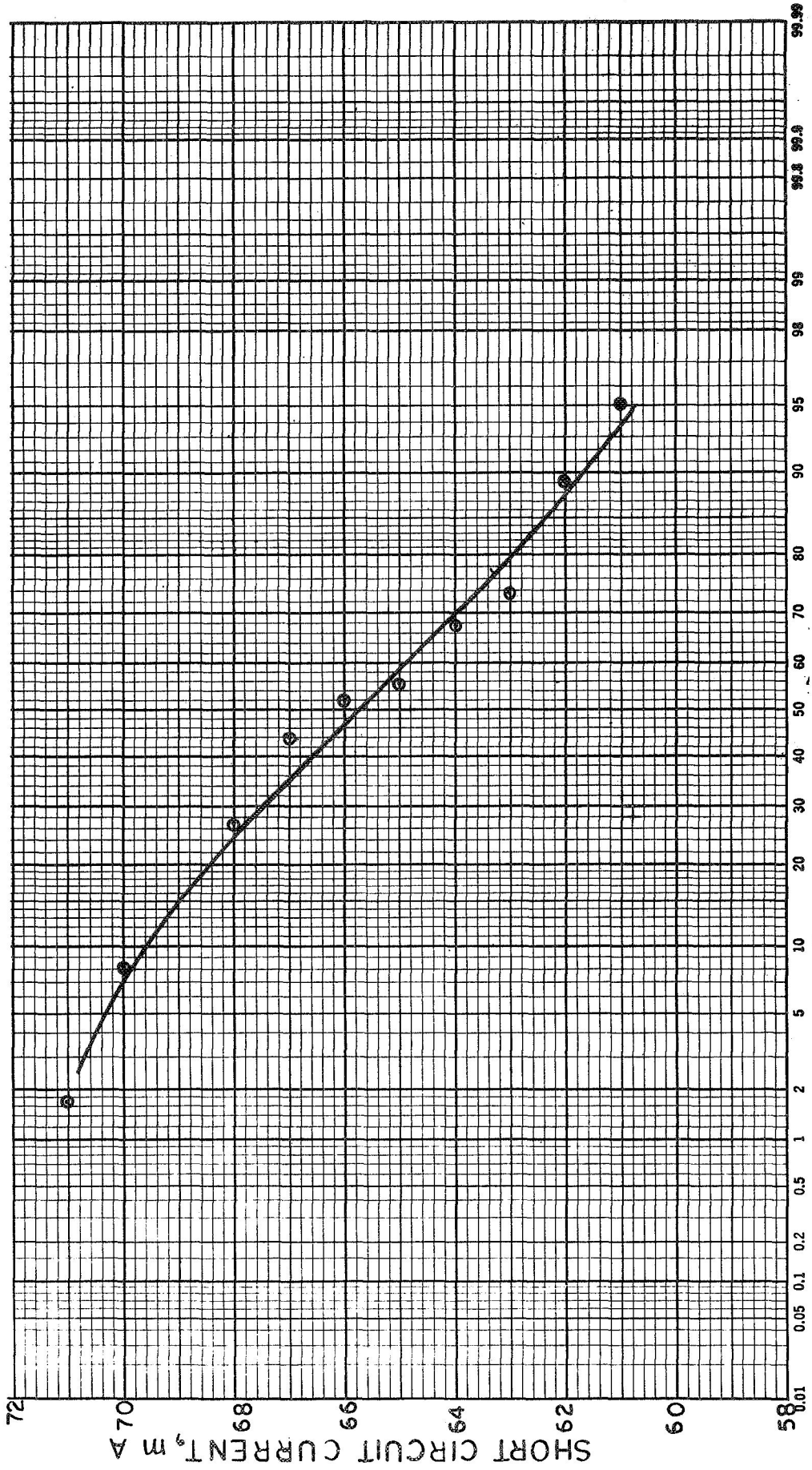

Figure 12. Short Circuit Distribution of Lithium Cells Fabricated for the Sixth Lot. 20 ohm cm crucible grown cells lithium diffused 90 minutes and redistributed 120 minutes at 425°C; measured at 25°C in solar simulator at 140 mW/cm^2.

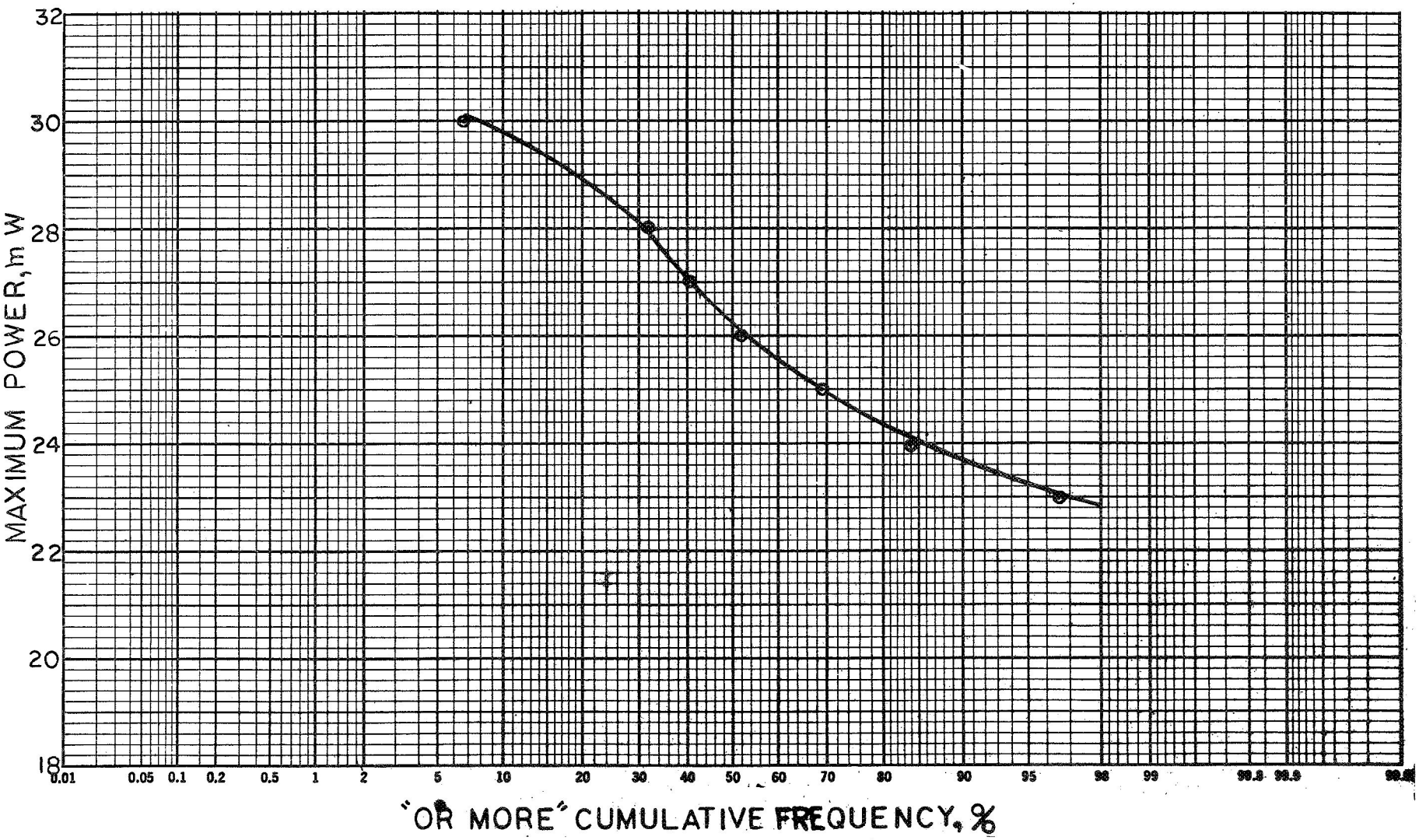

Figure 13. Maximum Power Distribution of Lithium Cells Fabricated for the Sixth Lot. 20 ohm cm crucible grown cells lithium diffused 90 minutes and redistributed 120 minutes at 425°C; measured at 25°C in solar simulator at 140 mW/cm^2.

Lot 7 consisted of 10 ohm cm float zone cells, lithium diffused 90 minutes and redistributed 120 minutes at 425°C. Figures 14 and 15 show the short circuit current and maximum power distributions for this lot of cells. The median short circuit current was 64.4 mA and the fifth to nintey-fifth percentile range was 68.5 to 59.9 mA. These particular diffusion parameters used for this lot of cells gave relatively high outputs for float zone lithium cells. The median output shown in Figure 15 is 26.5 mW with 5% of the cells having outputs ≥ 29.5 mW and 95% of the cells having outputs ≥ 23.5 mW.

Eight-hour diffusions at 325°C have been used for Lots 1, 3, and 4. Cells with this type of diffusion have been known to exhibit very high output. The short circuit current and maximum power distributions for the cells in Lot 1, 20 ohm cm float zone cells, are shown in Figures 16 and 17. The fifth to ninety-fifth percentile range for short circuit current is large with the 14.6 mA difference between 72.4 mA and 57.8 mA. The median output of this group of cells is 25.5 mW which is about 3.5% lower than the average output of 20 ohm cm float zone cells diffused 90 minutes and redistributed 60 minutes at 425°C. This may indicate that the eight hour lithium diffusion at 325°C is not optimum for float zone cells.

The short circuit current and maximum power distributions for Lot 3 are shown in Figures 18 and 19. These cells were fabricated from 20 ohm cm crucible grown silicon and the high outputs expected from an eight-hour diffusion at 325°C were observed. The distributions include only the 60 cells shipped to JPL, since a number of the cells had poor I/V curve shape due to contact shunting problems. Some of the cells with poor curve shape exhibited a dark characteristic curve which did not have exceptionally high dark reverse currents at 0.7 volts but did pass excess current at low voltages.

The spread in short circuit current for this lot is also large with a difference of 14.6 mA between the fifth percentile short circuit current (74.6 mA) and the ninety-fifth percentile short circuit current (60 mA).

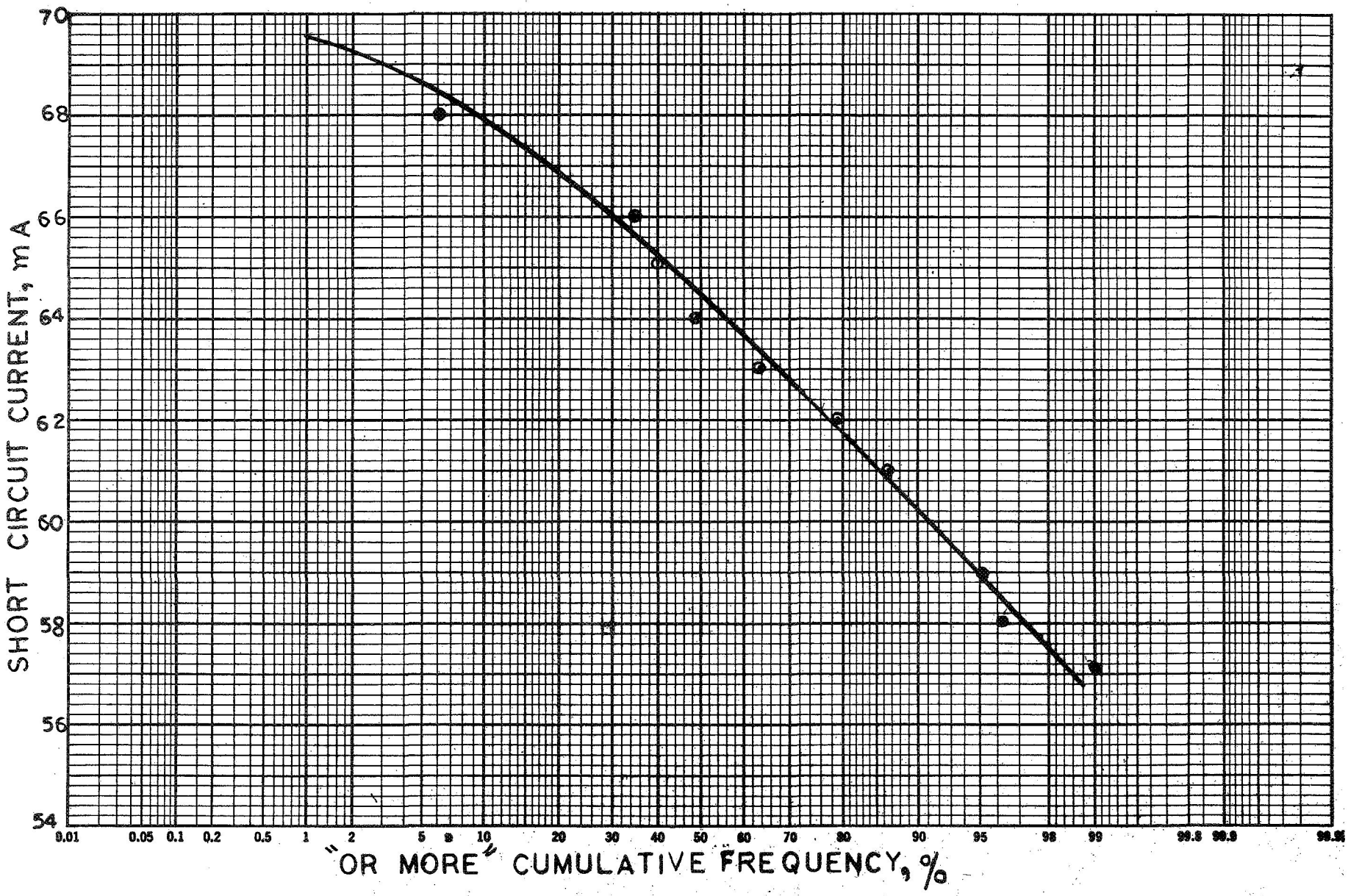

Figure 14. Short Circuit Current Distribution for the Seventh Lot 10 ohm cm float zone cells lithium diffused 90 minutes and redistributed 120 minutes at 425°C; measured at 25°C in solar simulator at 140 mW/cm^2.

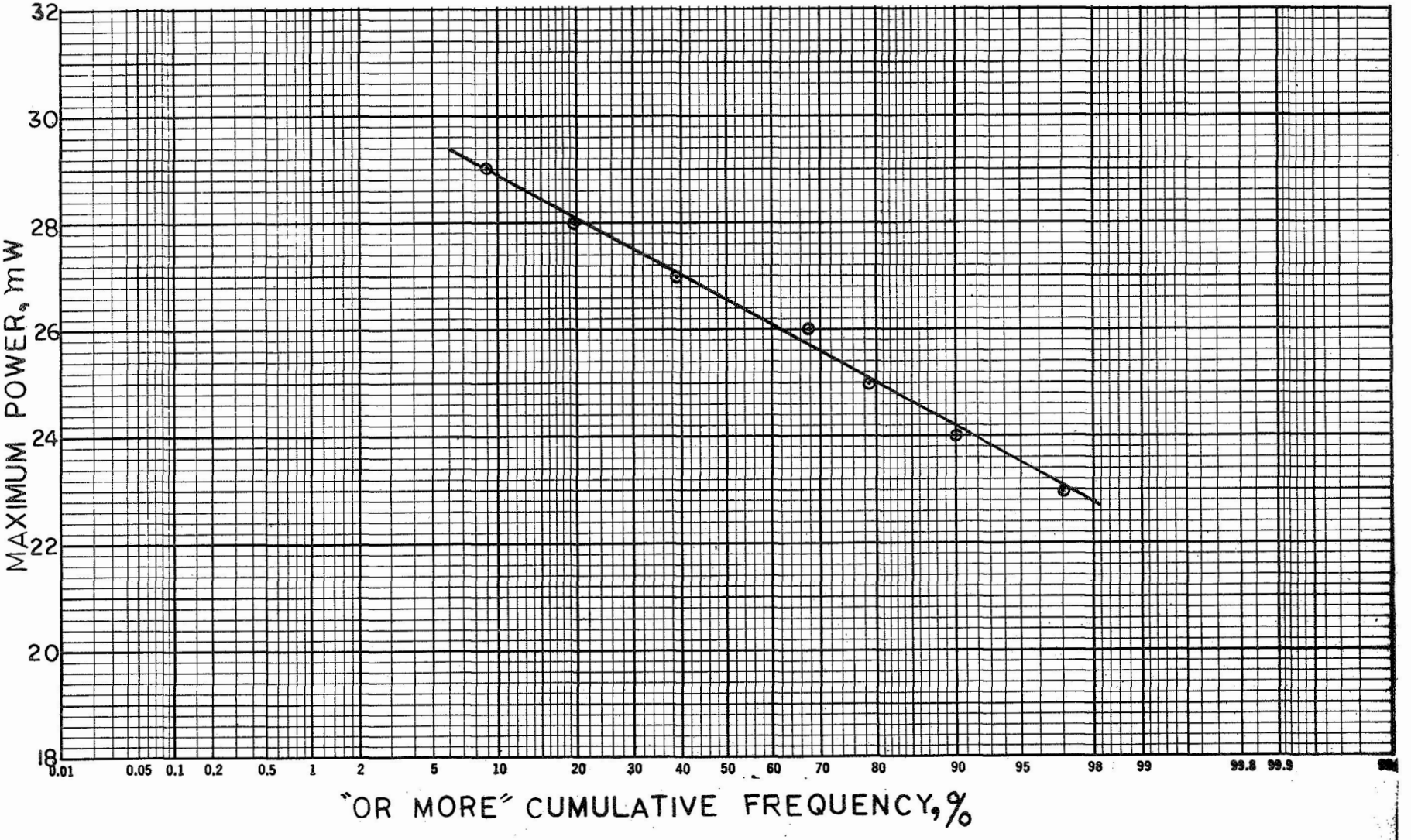

Figure 15. Maximum Power Distribution for the Seventh Lot.
10 ohm cm float zone cells lithium diffused 90 minutes and redistributed 120 minutes at 425°C; measured at 25°C in solar simulator at 140 mW/cm^2.

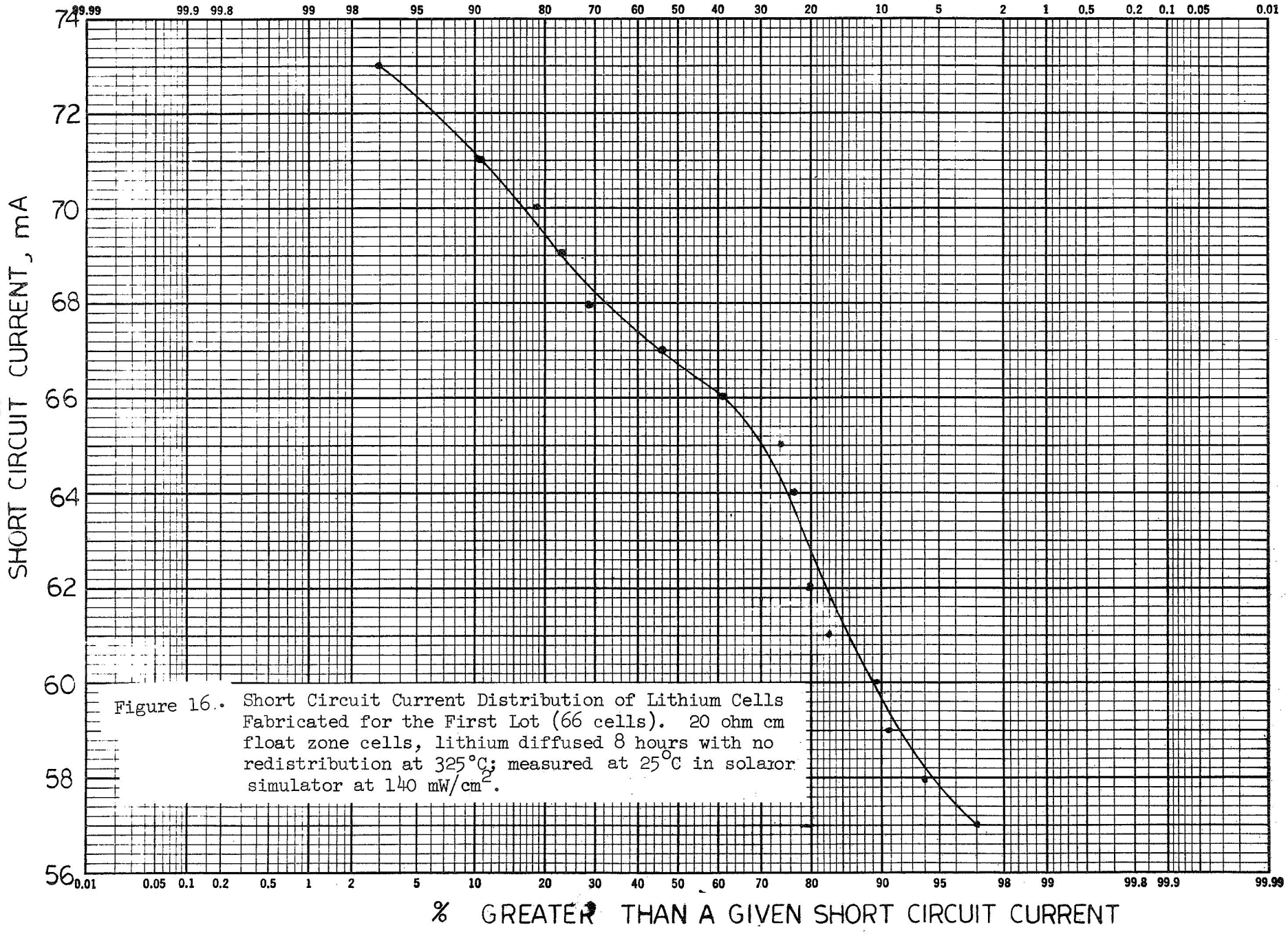

Figure 16. Short Circuit Current Distribution of Lithium Cells Fabricated for the First Lot (66 cells). 20 ohm cm float zone cells, lithium diffused 8 hours with no redistribution at 325°C; measured at 25°C in solaror simulator at 140 mW/cm^2.

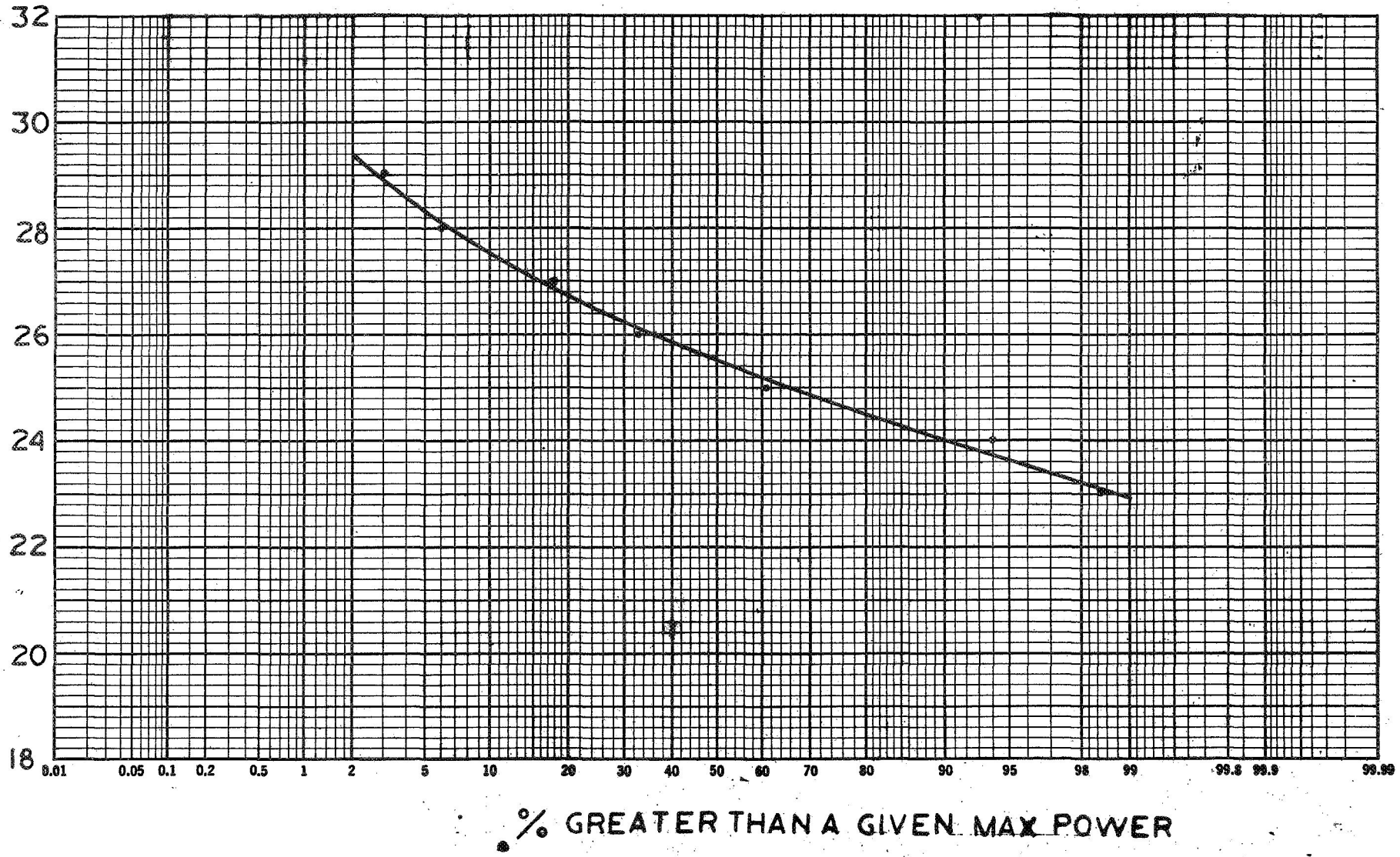

Figure 17. Maximum Power Distribution of Lithium Cells Fabricated for the First Lot (66 cells). 20 ohm cm float zone cells, lithium diffused 8 hours with no redistribution at 325°C; measured at 25°C in solar simulator at 140 mW/cm^2.

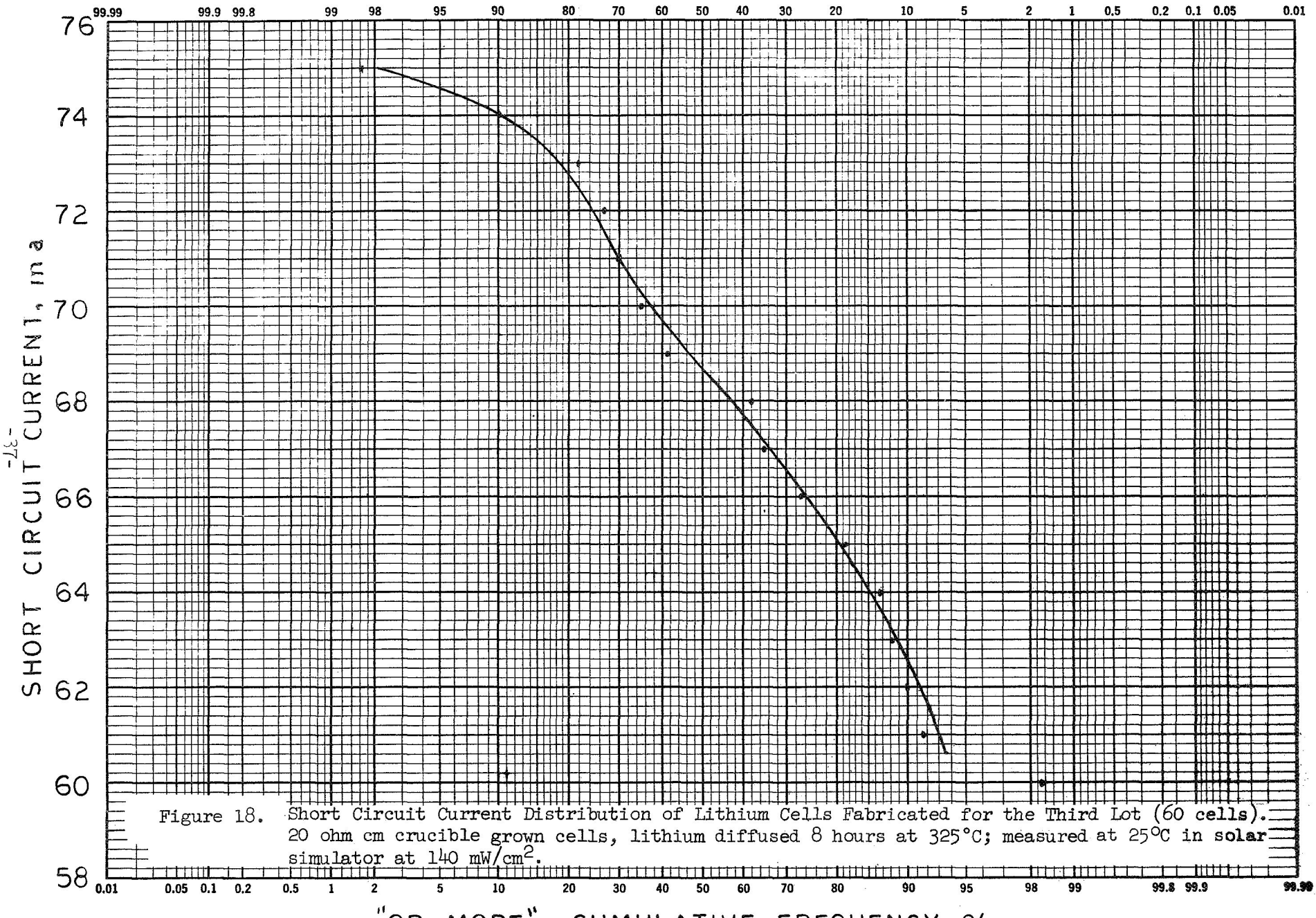

Figure 18. Short Circuit Current Distribution of Lithium Cells Fabricated for the Third Lot (60 cells). 20 ohm cm crucible grown cells, lithium diffused 8 hours at 325°C; measured at 25°C in solar simulator at 140 mW/cm^2.

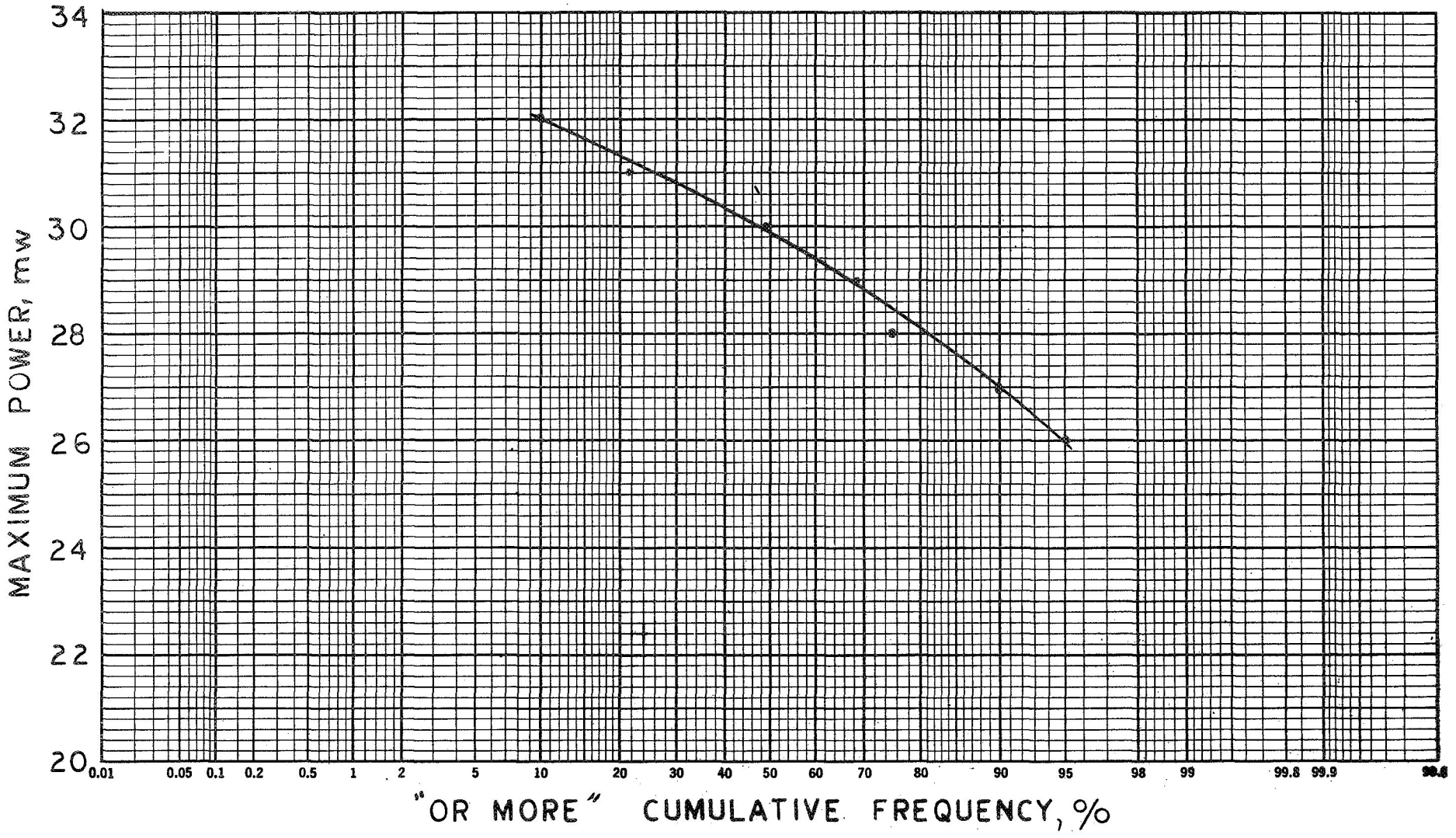

Figure 19. Maximum Power Distribution of High Output Lithium CG Cells. Lithium diffused 8 hours at 325°C with no redistribution TiAg Contacts, measured at 25°C in solar simulator at 140 mW/cm^2.

The maximum power distribution is narrow and high. The median output is 30 mW with 10% of the cells having outputs ≥ 32 mW and 90% having outputs ≥ 27 mW.

For Lot 4, 20 ohm cm float zone cells with an eight hour diffusion at 325°C were again fabricated. Compared to Lot 1, the short circuit current range for Lot 4 cells was smaller. However, the short circuit currents were also lower. As a result of the low short circuit current, these cells had low outputs. The entire distribution for Lot 4 was 2 mW lower than the maximum power distribution for Lot 1. Figure 20 compares the float zone cells in Lot 3 to the crucible grown cells fabricated for Lot 3. The median output of the crucible grown lithium cells was 6 mW higher than the median output of float zone cells fabricated for Lot 4. In terms of efficiency this corresponds to a median efficiency of 9% for the float zone cells and 11% for the crucible grown lithium cells. It is typical for crucible grown lithium cells to have higher outputs than float zone lithium cells, but usually the difference is 2 to 3 mW, or half an efficiency group. The low output of the float zone cells is typical of the losses observed when processing problems are encountered.

The short circuit current and maximum power distributions of all seven lots is summarized in Table II.

The crucible grown lithium cells diffused eight hours at 325°C which had such high initial outputs also had exceptionally high recovered outputs after being irradiated with 1 MeV electrons to an integrated flux of 3×10^{15} electrons/cm^2; (irradiations were performed and reported on by TRW Inc. under JPL Contract 952554). Figure 21 shows a cell with an initial output of 32.6 mW and a recovered output after irradiation of 21.9 mW. The cell shown in Figure 22 had a lower initial output, 29.4 mW, but it recovered to 23.5 mW. Figure 23 compares these two cells to a 10 ohm cm N/P irradiated to the same level. The output of the lithium cells is 11 to 20% higher than the output of the N/P. This increased efficiency and radiation resistance means that the lithium doped cells would be able to withstand about three times the radiation fluence for the same power output degradation when compared to the 10 ohm cm N/P solar cell.

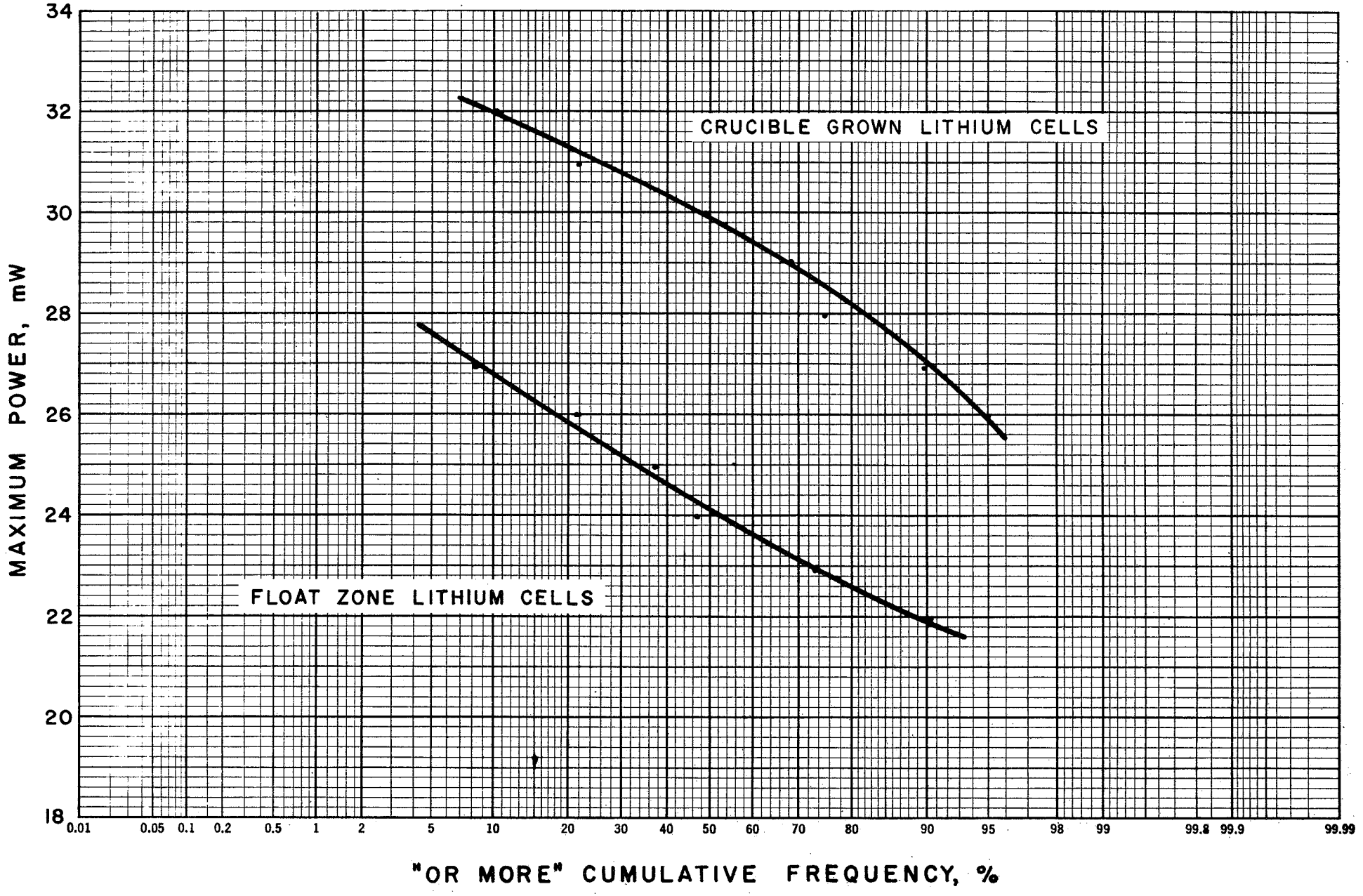

Figure 20. Comparison of Float Zone and Crucible Grown Lithium Cells Diffused 8 Hours at 325°C. Measured at 25 C in solar simulator at 140 mW/cm^2.

TABLE II

SUMMARY OF CELL LOTS DELIVERED TO JPL

Lot Number	Material Type and Resistivity	Lithium Diffusion, Redistribution, (min)	Temp. °C	Maximum Power, mW			Short Circuit Current, mA		
				5% of Cells ≥	50% of Cells ≥	95% of Cells ≥	5% of Cells ≥	50% of Cells ≥	95% of Cells ≥
1	20 ohm cm F.Z.	480	325	28.3	25.5	23.6	72.3	66.7	58.2
2	100 ohm cm Lopex	90, 120	425	28.3	25.4	22.8	70.6	63.9	59.5
3	20 ohm cm C.G.	480	325	32.4	29.5	26.0	74.5	68.6	60.5
4	20 ohm cm F.Z.	480	325	27.6	24.1	21.4	65.0	58.8	53.8
5	20 ohm cm F.Z.	60, 120	425	27.0	25.6	23.6	65.2	62.5	59.5
6	20 ohm cm C.G.	90, 120	425	30.3	26.2	23.2	70.3	65.7	60.8
7	10 ohm cm F.Z.	90, 120	425	29.5	26.6	23.5	68.6	64.4	59.0

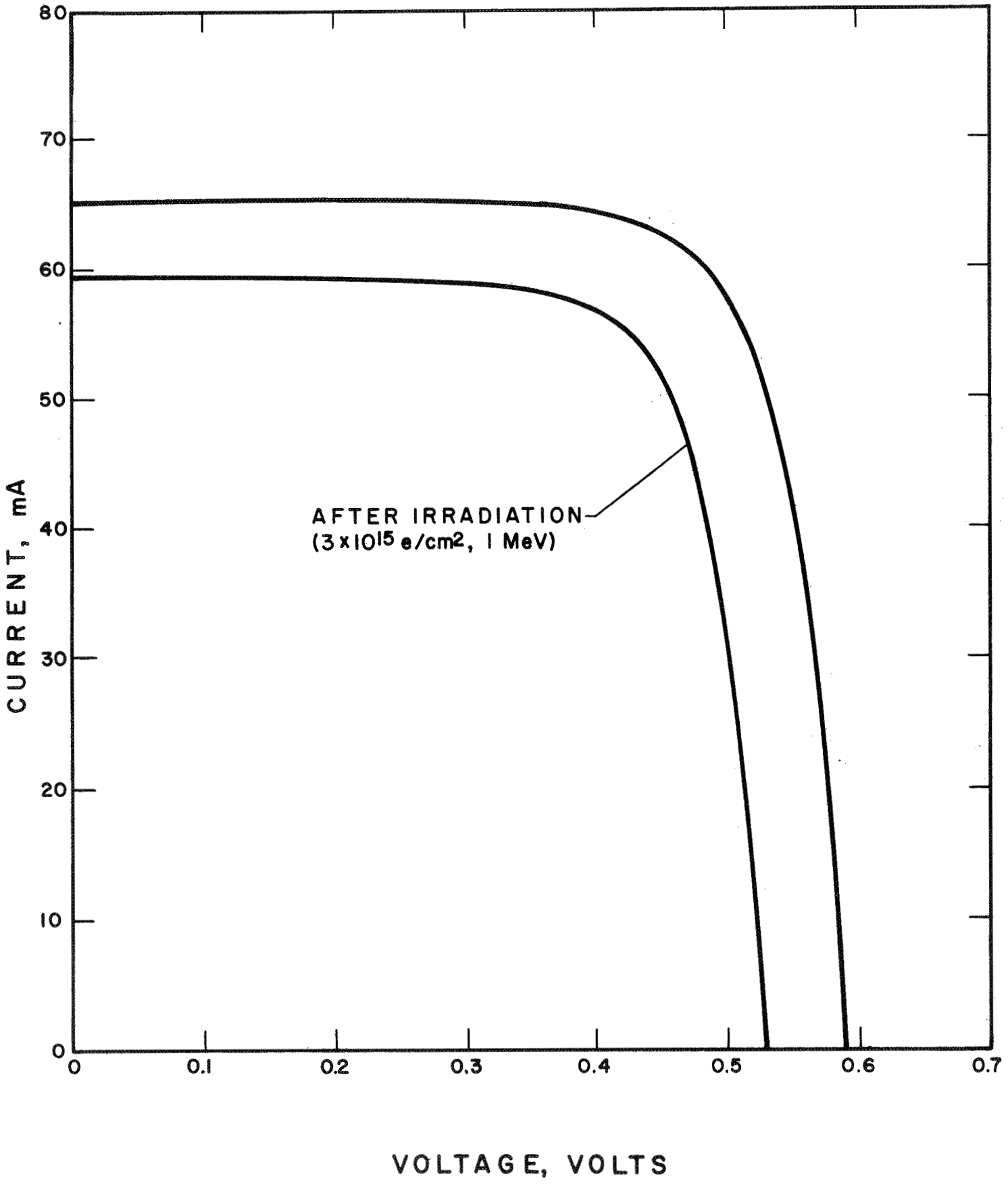

Figure 21. 20 Ohm cm Czochralski grown lithium cell before and after irradiation. Lithium diffused eight hours at 325°C; measured in Solar Simulator at 140 mW/cm^2.

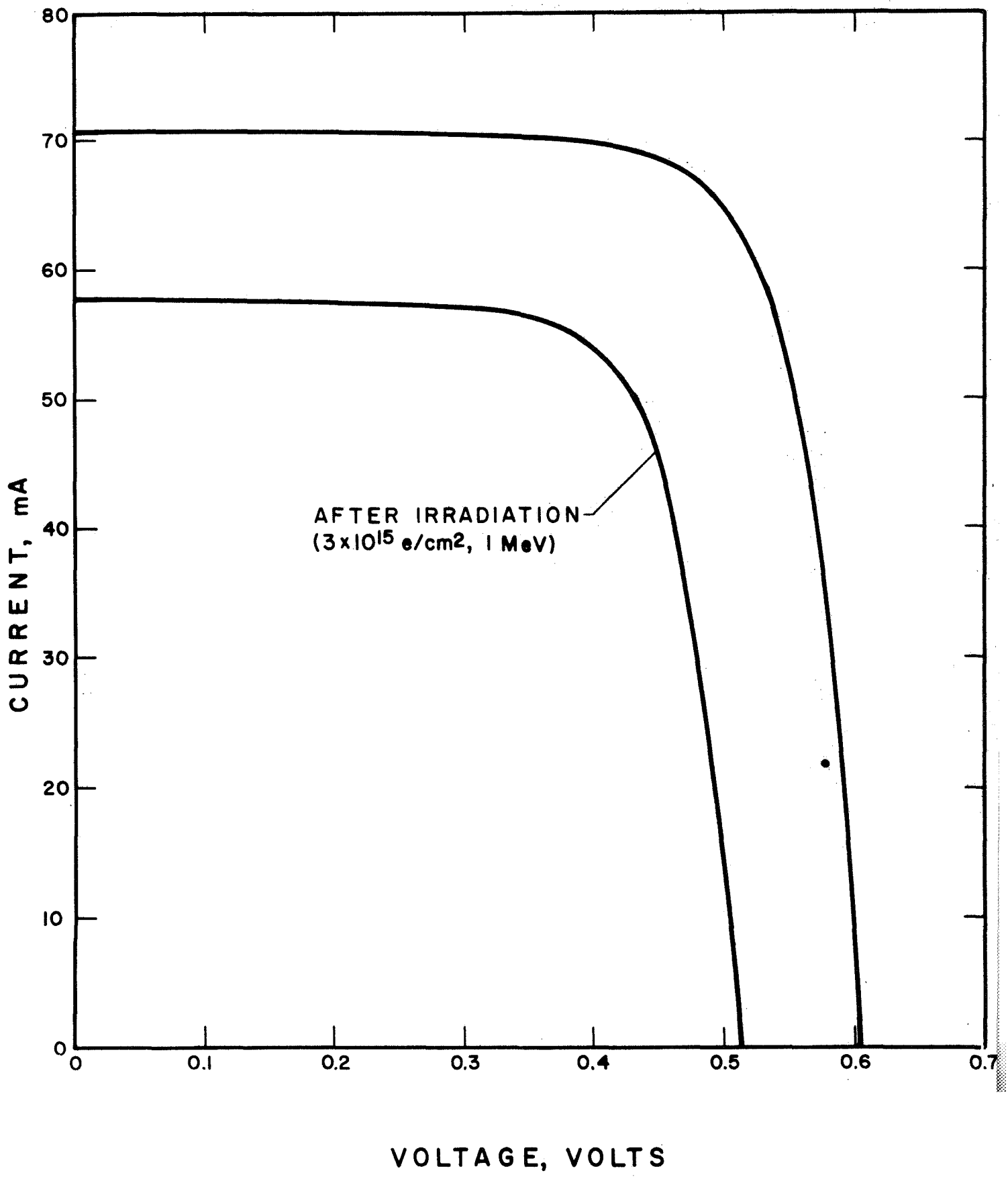

Figure 22. 20 Ohm cm Czochralski grown lithium cell before and after irradiation. Lithium diffused eight hours at 325°C; measured in Solar Simulator at 140 mW/cm^2.

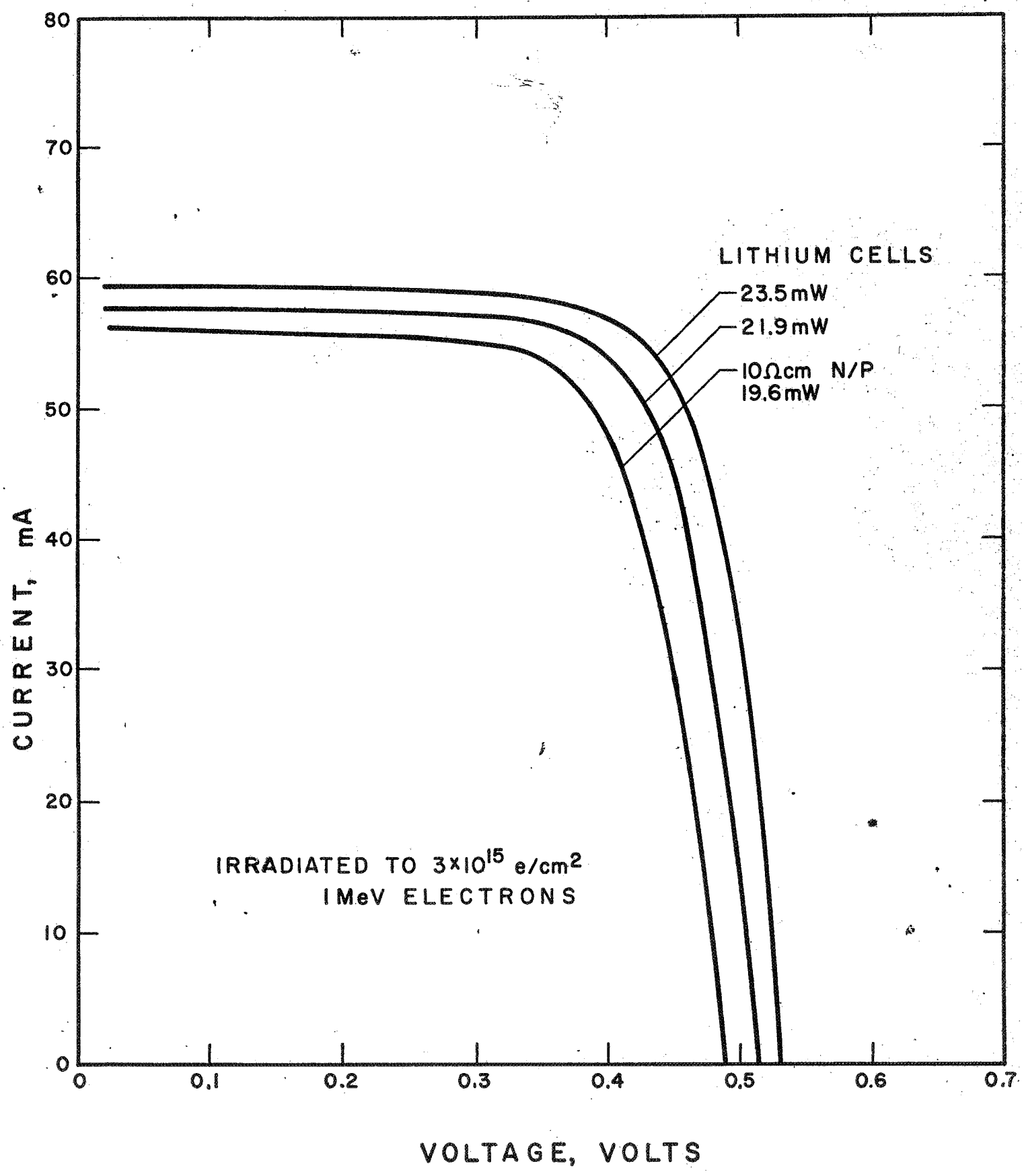

Figure 23. Lithium cells vs. 10 ohm cm N/P cell. Measured in Solar Simulator at 140 mW/cm^2.

3.0 CONCLUSIONS

Investigation of BBr_3 as an alternative boron diffusion source has resulted in cells with short circuit currents which were typically 5 to 10% lower than the short circuit currents of $BC\ell_3$ diffused cells. This did result in lower output cells (the efficiency of $BC\ell_3$ diffusion cells usually ranges from 11.0 to 12.5%); even so, efficiencies greater than 11.0% were obtained since the V_{oc} (608 mV) and fill factor (0.778) of the BBr_3 diffused cells were good. The stresses have been reduced and 0.006" thick 2 x 6 cm blanks can be diffused with no bowing.

Lithium concentration profiles can be obtained with an evaporated lithium layer which are comparable to those obtained by a painted-on lithium layer. High efficiency lithium cells can be made; however, comparison of the cumulative frequency distributions for cells with painted-on versus evaporated lithium layers, showed that there was more fall-off in cell output and, consequently, a larger percentage of lower output cells with the evaporated lithium. At a cumulative frequency of 90% there was a difference in output of about 1 mW.

Evaluation of the strength and humidity resistance of three contact systems--TiAg, TiPdAg, and Aℓ--which have been used on P/N lithium cells showed that the contact strengths were similar and the TiAg contact had the least humidity resistance. Contact strengths were evaluated by soldering or ultrasonically welding tabs to the contacts and pulling at a 90° angle until failure. Failures at less than 500 grams pull due to silicon fractures occurred with 40% of the cells. This was unusual since conventional N/P cells withstood 500 grams pull unless the contact is weak and peels. It is presumed to be indicative of the stresses present in P/N lithium cells, and is probably due to the boron diffusion since P/N cells without lithium which were tested also had failures due to silicon fractures at less than 500 grams. When the silicon did not fail the soldered bonds (on TiAg and TiPdAg contacts) exhibited more than 500 grams peel strength. The ultrasonically welded bonds

(on Aℓ as well as TiAg contacts) exhibited peel strengths greater than 150 grams and failure occurred when the (0.002" Aℓ) tab tore with the welded section remaining bonded to the contact. The peel strengths were comparable to those obtained with TiAg contacts on standard N/P cells.

When exposed to 95% relative humidity at 65°C and periodically tape tested for peeling, the TiAg front contacts peeled 100% after 200 hours, while the TiPdAg and Aℓ contact systems showed no degradation for the same period of exposure.

Since regions of the cell with no lithium could affect post radiation output, an experiment was performed to evaluate the effect of varying the percentage of undiffused region. Varying the undiffused regions from 0 to 50% did not affect the bulk resistivity or lithium concentration profiles of the diffused regions, nor did it affect electrical output. However, it is expected to influence the radiation recovery characteristic and these cells have been delivered to JPL for radiation testing.

A significant improvement in the efficiency of crucible grown lithium cells was made with a lithium diffusion schedule of eight hours at 325°C. Lot 10 fabricated during the previous contract had shown the highest outputs with 10% of the cells having outputs ≥ 30.4 mW, 90% of the cells having outputs ≥ 26.1 mW and a median output of 28.3 mW. Ten percent of the crucible grown lithium cells diffused 8 hours at 325°C had outputs ≥ 32.0 mW, 90% had outputs ≥ 27.0 mW and the median was 30.0 mW (11% efficiency). This is a 6% improvement in the median output.

These crucible grown lithium cells also had higher efficiencies after irradiation with 1 MeV electrons to $3 \times 10^{15} e/cm^2$. The recovered outputs of 21.7 to 23.5 mW were 11 to 20% higher than the 19.5 mW average output of 10 ohm cm N/P cells. This increased efficiency and radiation resistance means that lithium doped cells would be able to withstand about three times the radiation fluence for the same power output degradation when compared to the 10 ohm cm N/P solar cell.

4.0 RECOMMENDATIONS

The BBr_3 diffusion has made it possible to diffuse large area and thin cells; however, as the diffusion is presently done, silicon is etched and the diffusion cannot be used for special structure cells which require a non-etching boron diffusion source. Further boron diffusion investigation should be done in order to eliminate the etch reaction.

Once a non-etching boron diffusion source is obtained, work can be done on P/N^+N cell structures which would be designed with a stable N^+ region at the junction in order to obtain and maintain good junction characteristics as lithium combines with radiation induced defect sites.

Oxygen concentration is an important factor in recovery rate of lithium cells after irradiation and, therefore, studies should be performed to evaluate the performance of crucible grown lithium cells with various oxygen concentration levels. These studies might indicate an optimum oxygen concentration.

Additional cells with an eight-hour lithium diffusion at 325°C should be fabricated and made available to radiation laboratories. These cells have shown the best initial and recovered efficiencies and, therefore, the performance level of these cells should be determined on a statistical basis.